Journal of Power Sources 237 (2013) 243–259

Contents lists available at SciVerse ScienceDirect

Journal of Power Sources

journal homepage: www.elsevier.com/locate/jpowsour

Review

Fabrication and modification of solid oxide fuel cell anodes via wet impregnation/infiltration technique

Zhangbo Liu [a,b,1], Beibei Liu [a,1], Dong Ding [b], Mingfei Liu [b], Fanglin Chen [c], Changrong Xia [a,*]

[a] CAS Key Laboratory of Materials for Energy Conversion, Department of Materials Science and Engineering, University of Science and Technology of China, Hefei, 230026 Anhui, China
[b] School of Materials Science and Engineering, Center for Innovative Fuel Cell and Battery Technologies, Georgia Institute of Technology, 771 Ferst Drive NW, Atlanta, GA 30332, USA
[c] Department of Mechanical Engineering, University of South Carolina, Columbia, SC 29208, USA

HIGHLIGHTS

- Application of impregnation/infiltration in anodes is reviewed.
- Introducing nanoparticles to anodes by impregnation/infiltration is reviewed.
- Novel anodes by impregnation/infiltration are reviewed.
- Improved carbon and sulfur tolerance by impregnation/infiltration is reviewed.
- Enhancing anodic activity by impregnation/infiltration is reviewed.

ARTICLE INFO

Article history:
Received 29 October 2012
Received in revised form
4 March 2013
Accepted 6 March 2013
Available online 9 April 2013

Keywords:
Impregnation
Infiltration
Nanoparticles
Anode
Solid oxide fuel cell

ABSTRACT

The future commercialization and application of solid oxide fuel cell (SOFC) technologies requires the development of novel anode materials with excellent performance and stability at intermediate-temperatures with various fuels including hydrogen, syngas and particularly hydrocarbons. Whether by modifying the state-of-the-art Ni based anodes, or through exploring alternative metal cermet or ceramic based materials, wet impregnation/infiltration is shown to be one of the most effective approaches for both cell fabrication and performance optimization. This paper reviews most of the progress reported in the literature committed to the fabrication and optimization of SOFC anodes by wet impregnation for low temperature and/or hydrocarbon operation. The optimization of traditional nickel based anodes by adding excellent catalyst, the replacement of nickel by other inert metal or ceramic species, and some metal supported designs with impregnated catalyst are all presented and discussed, mainly focusing on the cell performance, redox and thermal stability, long-term reliability, carbon and sulfur tolerance of the anodes.

1. Introduction

The development of fuel cell technologies attracts increasing number of attentions since such devices can directly convert the chemical energy of fuels into electrical energy with very high efficiency. Besides, due to the low emissions of nitric oxides, sulfur oxides or particulate pollutants, fuel cells work more environmentally friendly than other power-generating systems. Among various kinds of fuel cells, solid oxide fuel cell (SOFC) is considered to be the most promising candidate to moderate the rapid increasing power requirements for the future development of human society and to minimize the fossil fuel consumption due to its excellent fuel flexibility over other types of fuel cells. In principle, any combustible fuels including hydrogen, syngas, ammonia and various gaseous or liquid hydrocarbons such as nature gas and ethanol can be used in SOFC systems for power generation. Moreover, the high temperature operation (usually at 600–1000 °C) of SOFC makes it feasible to utilize the waste heat, thus higher fuel efficiency could be expected.

Basically, each SOFC single cell consists of at least three components: a porous cathode where the oxygen molecules are reduced by electrons to oxygen anions, a dense electrolyte membrane which separates the porous electrodes and transports the

* Corresponding author. Tel.: +86 5513607475; fax: +86 5513601592.
E-mail address: xiacr@ustc.edu.cn (C. Xia).
[1] These authors contributed equally to this work.

0378-7753/$ – see front matter © 2013 Elsevier B.V. All rights reserved.
http://dx.doi.org/10.1016/j.jpowsour.2013.03.025

oxygen anions from the cathode/electrolyte interface to the anode side, and a porous anode where the diffused oxygen anions react with the fuels generating the electrons, which are subsequently transported through the external load back to the cathode chamber. Traditional SOFCs operate at temperatures as high as 800–1000 °C, with yttria-stabilized zirconia (YSZ), Ni–YSZ cermet, strontium-doped $LaMnO_3$ (LSM) as the typical electrolyte, anode and cathode materials, respectively. Such high operation temperature, unfortunately, significantly limits the materials selectivity and flexibility of cell components, leading to high cost of the SOFC systems. Thus, for the further development and commercialization of this clean and environmentally friendly technology, the operation temperature must be lower down from the traditional one to 700 °C or lower, so that the materials selectivity and flexibility could be greatly increased, and various metallic or ceramic materials with very low cost could be used as electrodes, interconnect, and manifolds of SOFC system with improved stability and reliability [1]. The overall cell performance of SOFC system, however, decreases significantly with the reduced operation temperature due to the enhanced polarization resistances derived from both electrodes and the decreased ionic conductivity of the electrolyte. The electrolyte resistivity could be reduced by utilizing anode or cathode supported cell design with very thin (e.g. 10–30 μm) electrolyte membrane [2,3]. Thus, the development of electrode materials with sufficient high performance and stability at intermediate temperatures is critical for the successful commercialization of SOFC technology.

Besides lowering down the operation temperature, another main requirement for SOFC commercialization is utilizing hydrocarbon fuels for operation. Although hydrogen is generally recognized as the most ideal fuel of the future, there are still lots of problems associated with the generation and storage of hydrogen which need to be overcome before its large-scale application. A major advantage of SOFC technology is its excellent fuel flexibility due to the fact that oxygen anions are the mobile species that transported from the cathode to the anode side through the electrolyte membrane, and the relative high temperatures operation makes it feasible to directly utilize hydrocarbons as the fuel without external reforming [4]. The state-of-the-art Ni–YSZ cermet anodes, unfortunately, are not stable in hydrocarbon fuels since Ni is an excellent catalyst for the formation of carbon fibers, and large amounts of carbon deposition would in turn lead to rapid degradation or even collapse of the cell performance by covering the catalytic actives sites, blocking the gas transportation as well as causing some cracks in the anode configuration [5–7]. In addition, sulfur species such as H_2S are widely found as impurities or additives in lots of commercial available hydrocarbon fuels, and their concentration may reach very high levels such as those in coal syngas and diesel. The traditional Ni-based anodes, however, also experience severe degradation with as low as ppm levels of H_2S [8]. Therefore, for the realization of direct hydrocarbon SOFCs, it is essential to develop alternative anode materials which could show sufficient high tolerance to carbon deposition and sulfur poisoning in hydrocarbon fuels.

In summary, the commercialization of SOFC technology mainly depends on the development of direct hydrocarbon SOFCs operating at intermediate temperatures with sufficient high performance and long-time stability, and the exploration of alternative electrode materials, especially novel anode materials with excellent coking and sulfur tolerance, is certainly the key step. There are basically two approaches to develop preferable electrode materials: optimizing the state-of-the-art electrode materials which have shown great performance at higher operation temperatures with hydrogen and syngas fuels, or exploring novel systems with high mixed ionic and electronic conductivity (MIEC). For the modification of traditional electrode materials, wet impregnation/infiltration has been shown to be a very effective way to enhance the so-called triple phase boundary (TPB) or to add various catalysts in the electrodes, thus improving the cell performance and reliability [9–13]. In addition, it is a perfect method to introduce novel electrode materials that could not be sintered at high temperatures due to its low melting point or poor thermal or chemical compatibility with other components into the pre-sintered framework to fabricate single cells [7,11–15]. Thus, it is one of the most promising techniques to design alternative electrodes for intermediate-temperature SOFCs (IT-SOFCs) with attractive fuel flexibility.

To date, there have been many studies toward SOFC electrodes modification or fabrication based on means of wet impregnation, and lots of attractive progress is obtained in the past decade. Since the commercialization of SOFC technology demands more on the anode materials with not only lower polarization resistance at reduced temperatures but also sufficient high coking and sulfur tolerance being required, in this paper, the progress that has been made on the modification and fabrication of anode structures using wet impregnation technique is briefly reviewed. The modifications of the state-of-the-art Ni-based anodes, the fabrication and applications of alternative copper or other metal and alloy based anodes, the investigations over various novel ceramic based anodes, and some designs of metal-supported cells with infiltrated anode functional layers are discussed in the following parts, mainly focus on the performance at intermediate temperatures, the coking tolerance in hydrocarbons, the stability in H_2S-containing fuels, as well as their tolerance to redox or thermal cycles.

2. Modification of traditional Ni-based anodes

As is mentioned above, Ni–cermet based anodes are the most commonly used anode materials for SOFCs, due to their excellent electrochemical catalytic activity for fuel oxidation reaction, sufficient high electrical conductivity, good stability and compatibility with YSZ and doped ceria (DCO) based electrolyte, and relatively low cost [16,17]. Introducing nanoparticles with high ionic conductivity and/or excellent catalytic activity is an effective approach to enhance the performance, tolerance and stability of the state-of-the-art Ni-based anode through wet impregnation technique.

2.1. Oxides impregnated Ni-based anode

Since YSZ and DCO are the most commonly used electrolyte materials and always act as the secondary phase in Ni–cermet anodes, nanoparticles with $Y_xZr_{1-x}O_{2-\delta}$ and $M_xCe_{1-x}O_{2-\delta}$ (M = Sm, Gd) formulae are naturally considered as the impregnation species in many studies. Jiang et al. compared the effect of YSZ and DCO impregnation on the microstructure and performance of Ni–YSZ anodes in hydrogen [10,18–20]. It was shown that both YSZ and DCO nanoparticles impregnation significantly inhibited the sintering, grain growth and agglomeration of YSZ and in particular Ni particles of the anodes [10,18]. The performance of the anodes for the hydrogen oxidation reaction was also substantially enhanced after the impregnation, i.e. after impregnation of ~8.5 vol% $Gd_{0.1}Ce_{0.9}O_{1.95}$ (GDC), the electrode polarization resistance of pure Ni anode decreased from 10.7 Ω cm^2 to 1.5 Ω cm^2 at 700 °C [10,19,20]. Impedance spectra results also showed that the anode behavior for the hydrogen oxidation reaction was clearly differentiated at low and high frequency, and the impregnation primarily decreased the resistance at high frequency, thus indicating that the main role of the impregnated

nanoparticles was to extend the TPB into the anode bulk. In addition, due to the higher ionic conductivity and catalytic activity compared with YSZ, DCO nanoparticles infiltration exhibits relatively better enhancement of the anode performance, thus attracting more detailed studies [21–26].

A theoretical model, which constructs the electrode as a sphere-packed framework whose surface is coated with nanosized second-phase particles as shown in Fig. 1a, is proposed by Zhu et al. to estimate the TPB length of nanoparticles impregnated electrodes [26]. Ding et al. further showed that the TPB length increases with the loading of coated nanoparticles, and is dependent only on the loading before a maximum loading for monolayer coverage is obtained [25]. In addition, the maximum loading increases with the porosity of the framework, so the prolonged TPB can be achieved by increasing the porosity of pre-sintered electrode framework and the loading of impregnation phase within the maximum amount, as shown in Fig. 1b. Timurkutluk et al. also proved that the electrode porosity and the impregnated GDC particle size significantly affected the cell performance [21]. Besides, they found that both too high molar concentration and too high temperature sintering of the infiltration solution would adversely affect the electrode performance, due to catalytic surface covering and grain growth, respectively. Any way, through careful and reasonable operation, ceria or DCO impregnated Ni–cermet anodes exhibited very high performance in hydrogen, even for cells with tubular structures [27,28] or cells with $La_{1-x}Sr_xGa_{1-y}Mg_yO_{3-\delta}$ (LSGM) electrolyte [22,23].

The performance and stability of ceria and DCO impregnated Ni–cermet anodes in hydrocarbon and H_2S containing fuels were also investigated. Wang et al. showed that GDC impregnated Ni anode was very stable when exposed to weakly humidified (~3% H_2O) methane at 800 °C, and the stability could be further improved by applying an anode current load of 20 mA cm^{-2} [29]. $Sm_{0.2}Ce_{0.8}O_{1.9}$ (SDC) impregnation can also enhance the cell

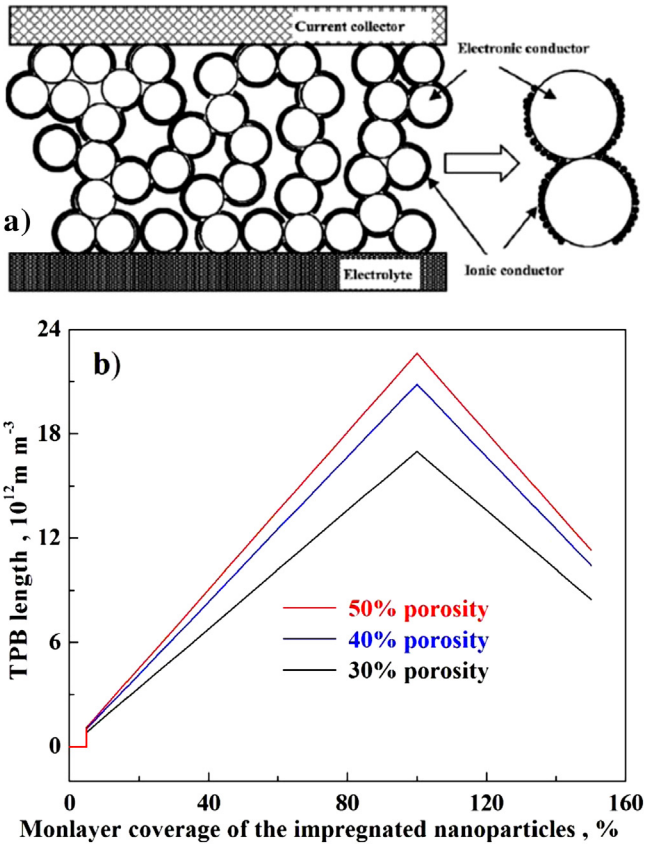

Fig. 1. Schematic diagrams of: a) a sphere-packed electrode coated by impregnated nanoparticles [26]; b) the correlation between the TPB length of the coated electrode and the loading of the nanoparticles by impregnation at different porosities [25].

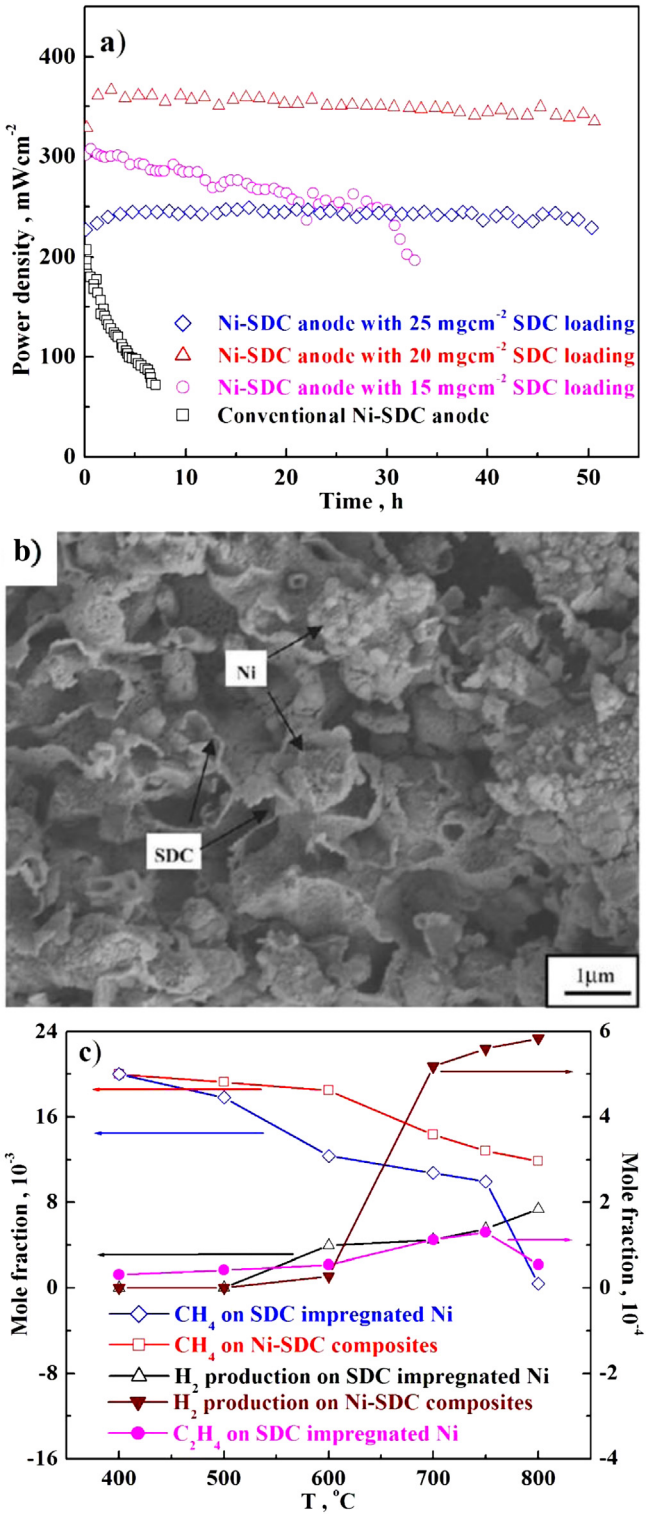

Fig. 2. a) Stability comparison for cells with different SDC loading in the Ni–SDC anodes, when operating at 600 °C in wet methane and b) a cross-section view of the anode with 20 mg cm^{-2} SDC loading after 50 h operation [30]; c) molar fractions of H_2, CH_4 and C_2H_4 when 2 mol% CH_4 catalytic decomposed on conventional Ni–SDC anode and SDC impregnated Ni-based anode at different temperatures [31].

performance and stability of Ni-based anode in wet methane [30]. As shown in Fig. 2a, the performance of conventional cell decreased very quickly in wet methane. In contrast, the cells with SDC impregnated anodes exhibited rather stable performance, and after 50 h operating, no visible carbon was found on the infiltrated anode surfaces (Fig. 2b). Liu et al. investigated the catalytic decomposition of methane on SDC impregnated Ni-based anode using the molecular-beam mass spectrometry coupled with tunable synchrotron vacuum ultraviolet photoionization [31]. They found that the coating of SDC nanoparticles not only decreased the decomposition temperature, but also increased the conversion ratio, thus being highly catalytic active for methane decomposition (Fig. 2c). In addition, C_2H_4 was observed when methane decomposed on SDC impregnated anodes, indicating that the SDC loading can suppress carbon deposition by the removal of C_2H_4. Besides methane, SDC impregnated Ni-based anodes also exhibited very stable performance without obvious degradation and carbon deposition for more than 260 h when *iso*-octane–air mixture was directly used as the fuel [32]. Chen et al. even found that some Ti doping of the SDC impregnation phase showed substantial effect on the electrochemical activity for methane oxidation, as these coated $Sm_{0.2}(Ce_{1-x}Ti_x)_{0.8}O_{1.9}$ species can enhance the kinetics of methane oxidation due to an improved oxygen storage capacity and redox equilibrium of the anode surface, in addition to effectively preventing the methane from directly impacting on the Ni particles [33]. The sulfur tolerance of Ni-based anodes can also be improved by ceria and DCO nanoparticles impregnation. As shown in Fig. 3, a cathode supported cell with ceria infiltrated Ni–YSZ anode delivered quite stable power density of 220–240 mW cm^{-2} for 500 h at 700 °C with humidified hydrogen fuel containing 40 ppm H_2S, while the performance of the un-impregnated cell dropped to 0 mW cm^{-2} in a few minutes [34]. $Mo_{0.1}Ce_{0.9}O_2$ impregnated Ni–YSZ anode was also proved to exhibit very good sulfur tolerance and coking resistance [35].

Besides YSZ, ceria and DCO, the impregnation of some other types of oxides can also enhance the performance and stability of Ni-based anodes. Liu et al. found that the impregnation of non-conductive samaria nanoparticles could enhance the performance of Ni–SDC anodes in hydrogen fuel as ceria and SDC particles with the same loading did, while inert alumina impregnation only had detrimental effects on the anodes, as shown in Fig. 4 [36]. Some

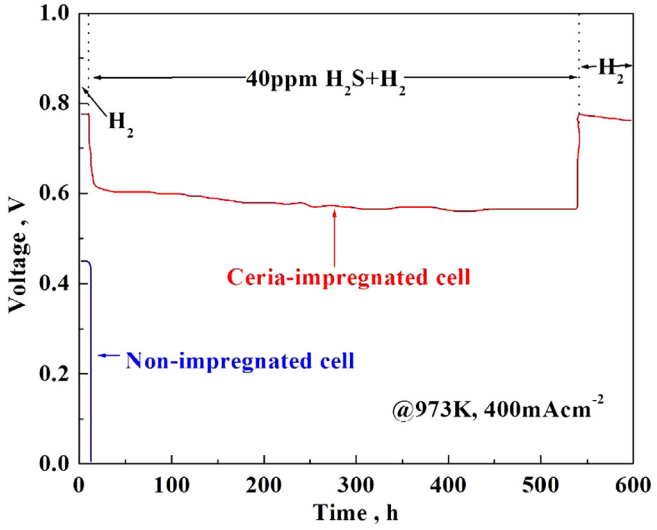

Fig. 3. Cell voltage as a function of time for cathode supported cells with and without ceria impregnation on the Ni–YSZ anodes exposed 40 ppm H_2S at 700 °C [34].

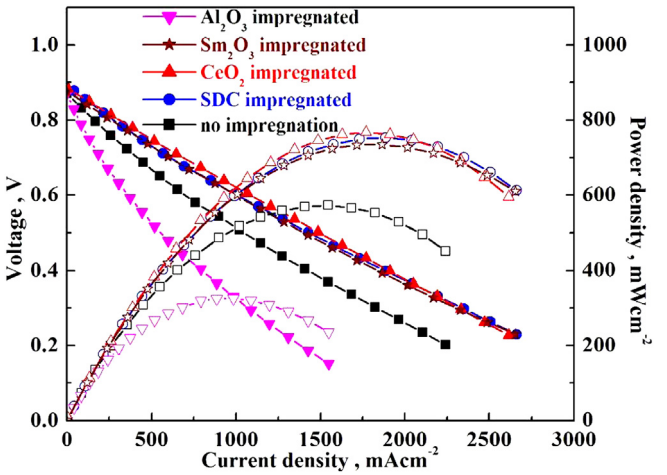

Fig. 4. Dependence of cell voltage and power density on current density for cells with 1.7 mmol cm^{-3} of various oxides impregnated Ni–SDC anodes operated in humidified hydrogen at 600 °C [36].

proton conductive perovskites, including $SrZr_{0.95}Y_{0.05}O_{3-\delta}$ [37,38] and $SrCe_{0.95}Y_{0.05}O_{3-\delta}$ [39], also exhibited substantial effects when impregnated into Ni-based anodes with hydrogen and in particular dry methane as the fuel, due to the increased oxygen coverage near the TPB and the enhanced production of water. Besides, BaO coating also significantly improved the sulfur tolerance of Ni–YSZ anodes due to its high water adsorption ability [40].

2.2. Metal optimized Ni-based anode

Besides various oxide materials, the impregnation of some metal especially precious metal species can also enhance the performance and stability of Ni-based anodes. Babaei et al. systematically investigated the electrocatalytic promotion effect of palladium nanoparticles on hydrogen oxidation on Ni–GDC anodes [41,42]. They showed that when hydrogen was used as the fuel, the electrode polarization resistance was significantly decreased with the presence of Pd nanoparticles in the anode, and the major function of these nanoparticles was to decrease the electrode impedance associated with the adsorption and diffusion processes [42]. The significantly enhanced adsorption and diffusion processes of the impregnated Pd nanoparticles were considered to be related to the significantly promoted hydrogen and oxygen spillovers over the Pd/PdO redox couple and hydrogen permeability through the Pd phase as shown in Fig. 5a. Also, they proved that a synergetic effect can be developed to further decrease the polarization resistance against both adsorption/diffusion and charge transfer step of the reaction by combining the catalyst impregnation with incremental application of bias current on the anode [41]. When operated in methane and ethanol fuels, the electrode polarization resistance was also substantially reduced, but the carbon deposition cannot be completely suppressed by the impregnation of Pd nanoparticles [42]. It was also reported that Pd impregnation significantly enhanced the sulfur tolerance of Ni–GDC anodes particularly when the H_2S concentration was less than 100 ppm, most likely due to the significant promotion effect on the hydrogen dissociation and surface diffusion processes, as well as reduced detrimental effect on the morphology and microstructures of Ni and GDC phases of the anodes [43]. However, as shown in Fig. 5b, due to the aggregation and growth of impregnated Pd nanoparticles, the sulfur poisoning effect cannot be completely inhibited.

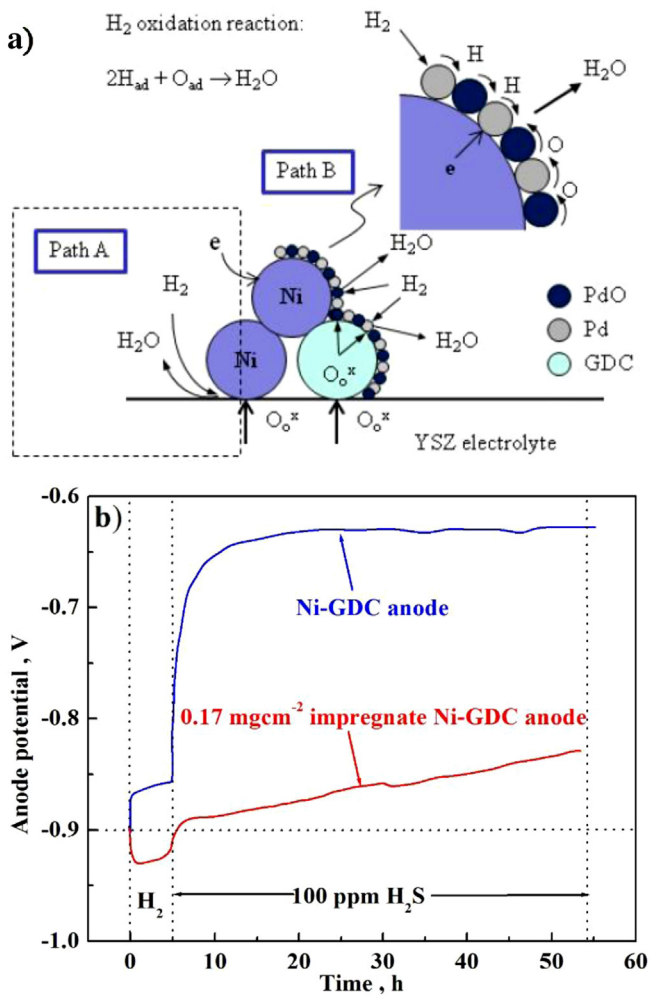

Fig. 5. a) Schematic diagram of the electrocatalytic of the Pd/PdO redox nanoparticles on the hydrogen oxidation reaction on Ni–GDC anodes [41,42]; b) polarization performance of Ni–GDC and 0.17 mg cm^{-2} Pd impregnated Ni–GDC anodes in 100 ppm H_2S containing H_2 measured at 200 mA cm^{-2} and 800 °C [43].

Gavrielatos et al. showed that 1% (atomic ratio) Au with respect to Ni modified Ni–YSZ anodes were highly tolerant to carbon decomposition, even at methane to water ratio as high as three [44]. Actually, some less expensive metals, such as copper and iron, can also be introduced to modify Ni-based anodes. When copper nanoparticles were uniformly distributed on the surface of Ni–SDC matrix through impregnation, the cell stability in methane fuel was significantly improved, with only ~2% loss after 12 h operation [45]. Armstrong et al. even proved that single cell with a dual-layer anode consisting of a Cu–ceria impregnated Ni–YSZ support outer layer and a Ni–YSZ electroactive inner layer could exhibit high electrochemical performance without evidence of anode coking for the direct operation on ethanol [46]. A recent study showed that with iron impregnating into Ni–YSZ/Ni–ScSZ anodes, the cell performance with ammonia fuel was improved, even comparable to that with hydrogen fuel [47].

2.3. Nickel introduction by infiltration technique

In addition to loading various oxide and/or metal phases for modification, it is also reasonable and feasible to introduce nickel itself to fabricate Ni–cermet anodes with improved performance and stability. For traditional Ni–cermet anodes, the nickel content must be no less than 30 vol% to ensure sufficient high electronic conductivity on the basis of a percolation model [48]. Such high Ni content may lead to cracks or warps of the electrolyte/anode composites during co-sintering because of different thermal expansion coefficients (TECs) [49]. On the other hand, while experiencing reduction–oxidation (redox) cycles, the traditional Ni–cermets are subjected to intense volume changes which may cause the destruction of the thin electrolyte membrane or cermet structure.

When nickel nanoparticles were impregnated into pre-sintered YSZ or DCO backbones, much lower Ni content with finer distribution was required to provide adequate electrical conductivity of the anodes [50–52]. Accordingly, lower values of TECs, which were much closer to that of the electrolyte, were obtained for the anodes prepared by impregnation method [53]. Moreover, due to the fine-grained microstructures and a homogenous distribution of Ni nanoparticles, the anodes prepared through impregnation were more easily reducible than those prepared by other methods [54]. More importantly, the Ni-impregnated anodes exhibited excellent redox [55–57] and long time [58] stability, as shown in Fig. 6. Another superiority of Ni impregnated anodes is their feasibility to fabricate cells with thin film LSGM electrolyte, since the severe reaction between LSGM and NiO at high temperature can be avoided [59,60].

The subsequent loading of some additives can further enhance the quality of Ni impregnated anodes. As proved by Qiao et al., ceria addition enhanced the Ni nanoparticles dispersion on YSZ framework [51]. Low conductivity degradation rates of Ni impregnated YSZ anodes were observed with the following infiltration of various sintering inhibitors, including MgO, Al_2O_3, TiO_2, CeO_2 and GDC [61]. As shown in Fig. 7, the best inhibitor effect was obtained with higher loadings of GDC, and CeO_2 impregnation showed a similar potential. An adverse effect observed for MgO, Al_2O_3 and TiO_2 loaded anodes was the reduced conductivity, possibly due to the reaction with Ni that formed higher resistive phases. Good anchoring effects with not only decreased degradation rates under high temperature thermal treatment but also increased initial performance levels were shown when metastable Al_2TiO_5 was added to the YSZ framework of Ni impregnated anodes [62].

Hydrocarbon fuels such as methane and methanol were also successfully applied on these Ni impregnated anodes. With Ni–CeO_2 mix-impregnated YSZ anodes, the cell performance was improved with increased CeO_2 content, especially when methane was used as the fuel, as shown in Fig. 8 [63]. Besides, it was also proved that anodes calcined at higher temperature exhibited better stability than those calcined at lower temperature. The catalytic properties of Ni impregnated $Y_xCe_{1-x}O_{2-\delta}$ (YDC) electrodes were investigated for partial oxidation of methane [64]. In the temperature range of 600–850 °C, Ni–$Y_{0.1}Ce_{0.9}O_{1.95}$ catalyst exhibited great catalytic activity for methane conversion, CO selectivity and H_2 selectivity, with the H_2/CO molar ratio in the products very close to the theoretical value of 2. The direct utilization of methanol on Ni and Ni–$Zr_{0.35}Ce_{0.65}O_{2-\delta}$ (ZDC) impregnated YSZ anodes were investigated by Cimenti et al. [65]. As shown in Fig. 9, performance and stability were improved by the presence of ZDC, although carbon formation was not entirely avoided. The study showed that, in addition to increasing the conductivity within the anodes, the presence of ZDC also influenced the types of carbon that formed, which were more reactive and could be removed without complete destruction of the anode microstructure. Thus, the structure integrity of Ni–ZDC impregnated YSZ anodes was maintained and the performance was not negatively impacted.

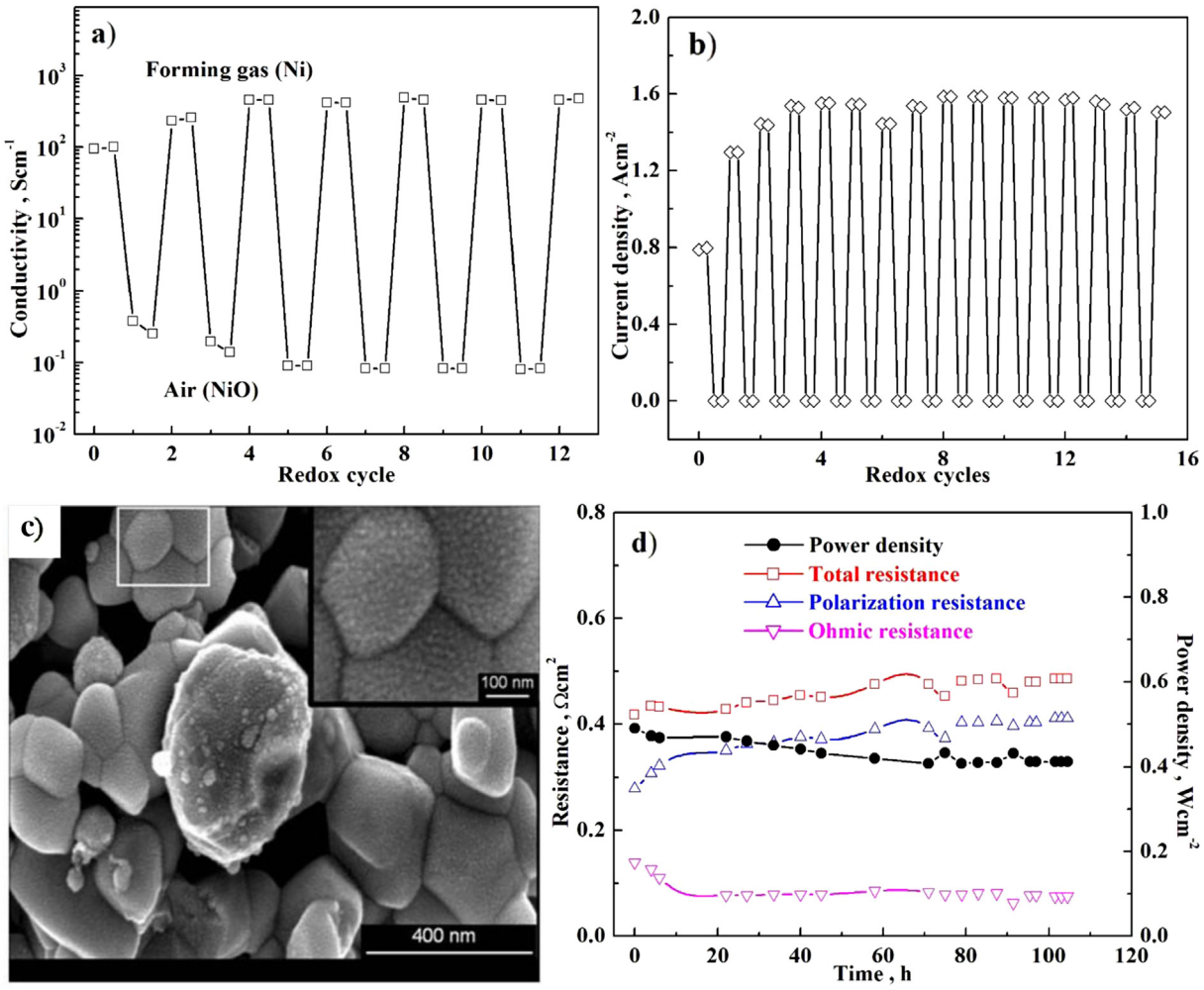

Fig. 6. a) Redox cycle test for Ni polymer precursors impregnated YSZ anodes in air-forming gas atmosphere at 700 °C [55]; b) influence of redox cycles on the current density of Ni impregnated YSZ anodes at short circuit conditions at 800 °C [57]; c) scanning electron micrograph of the Ni coated YSZ anodes after 15 redox cycles at 800 °C [57]; d) influence of short circuit operation time on the ohmic resistance, polarization resistance, total resistance and power density for cells with nanocomposite Ni–YSZ anode and LSM–YSZ cathode operated at 800 °C [58].

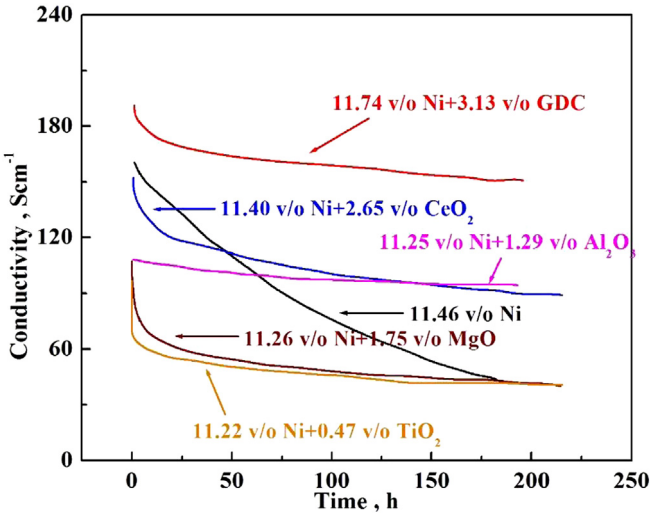

Fig. 7. Conductivity degradation of Ni impregnated YSZ anodes with various sintering inhibitor candidates measured at 650 °C [61].

3. Replacing Ni with Cu or other metals for hydrocarbon utilization

Since nickel itself is highly active toward carbon deposition and sulfur poisoning in hydrocarbon fuels, another sensible strategy to develop direct hydrocarbon SOFC anodes is totally replacing nickel with other highly conductive metal or oxide materials which do not catalyze the formation of carbon fibers and detrimental sulfur species in the way that nickel does. These potential alternatives, however, may have other drawbacks, such as low melting point, TEC mismatch with commonly used electrolyte materials, insufficient catalytic activity toward fuel oxidation, etc., which may cause serious issues to the cell fabrication and application. Wet impregnation is just a perfect way to solve these problems as this technique can add both dispersed and contiguous nanoparticles in SOFC electrodes at reduced temperatures [66]. In this section, we will discuss the studies with copper and other metals or alloys as anodes for IT-SOFCs, in particular direct carbon SOFCs.

3.1. Cu-based anodes

Due to its good electrical conductivity, low activity toward hydrocarbons as well as very low cost, Cu is widely considered as

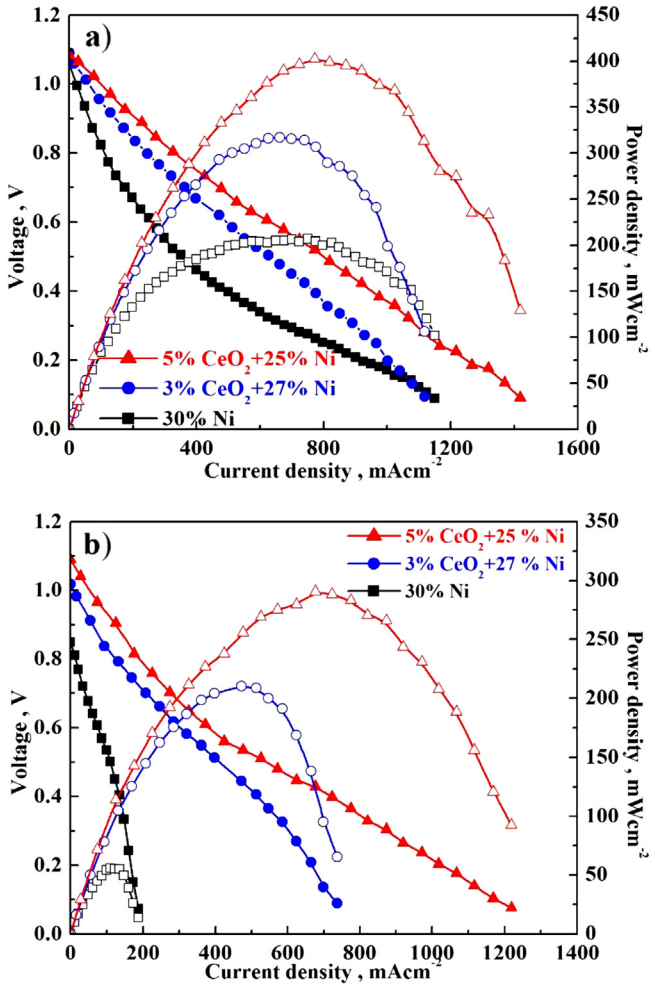

Fig. 8. Dependence of cell voltage and power density on current density for cells with Ni–CeO_2 impregnated YSZ anodes with different ratio of Ni:CeO_2 tested at 800 °C in: a) humidified (3% H_2O) hydrogen and b) dry methane fuels [63].

a good alternative of Ni in SOFC anodes. The melting point of either Cu or copper oxides, however, is much lower than the typical densification temperatures of electrolyte membranes (usually >1300 °C), making it difficult to fabricate high performance anode supported designs using conventional co-sintering processes. Thus, the universal way to fabricate Ni-free Cu-based anodes involves impregnating Cu precursor solution into pre-sintered highly porous YSZ or DCO framework on the dense electrolyte and subsequent reduction of the loaded copper oxides.

The first attempt was conducted by Craciun et al. through impregnating Cu and Ni nitrate salts into porous YSZ films prepared using a mixture of zircon fibers and normal YSZ powders [67]. While working on a 230 μm thick YSZ electrolyte with H_2 as the fuel, the current–voltage (I–V) curves for either the Cu or Ni impregnated anodes were found to be identical to those of the Ni cermets formed using the traditional method. In addition, it was shown that the addition of ceria by impregnating $Ce(NO_3)_3$ led to additional increase of the cell performance. When dry methane was applied, these Cu–YSZ anodes were essentially inert for coking, and the addition of ceria gave rise to reasonable power densities and stable operation over a period of at least three days [68]. The major carbon-containing product was CO_2, with only traces of CO observed, and excellent agreement between the actual cell current

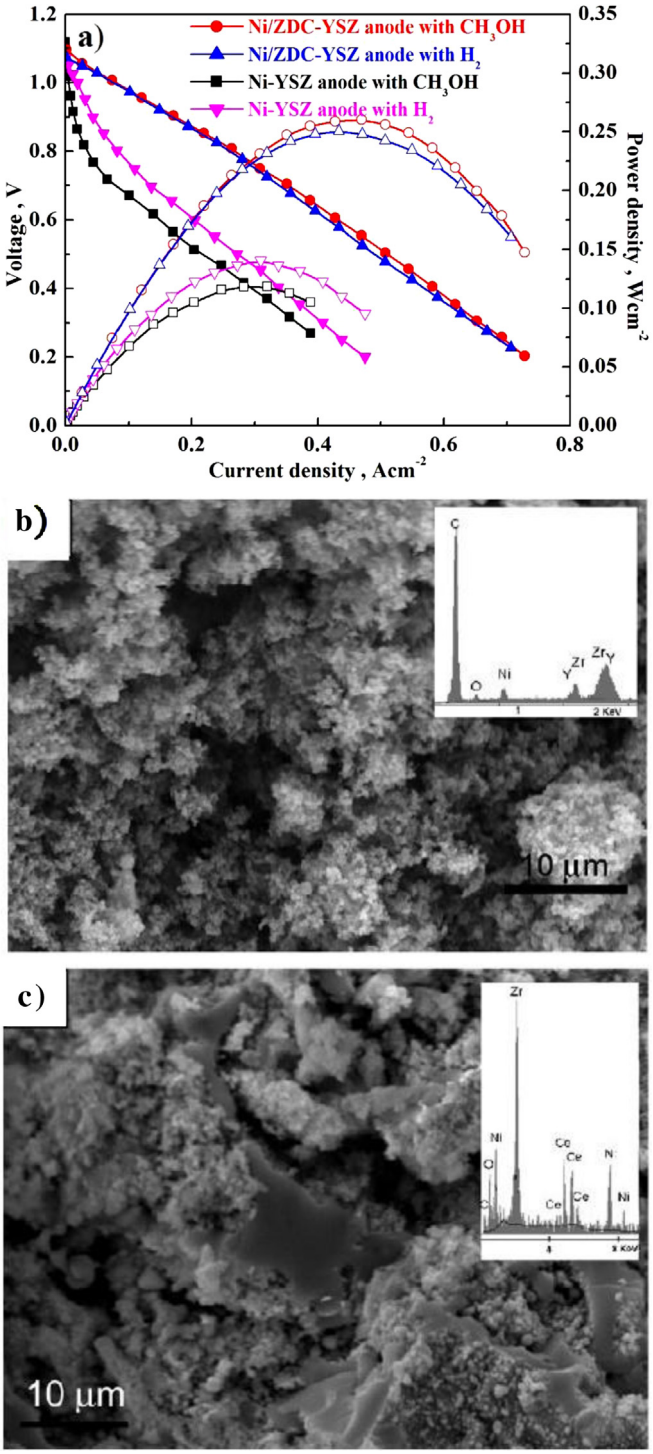

Fig. 9. a) Dependence of cell voltage and power density on current density for cells with Ni and Ni/ZDC impregnated YSZ anodes tested at 800 °C with wet hydrogen and methanol fuels; b) surface view of Ni impregnated YSZ anode after 12 h exposure to methanol at OCV; c) surface view of Ni/ZDC mix-impregnated YSZ anode after 12 h exposure to methanol at OCV. EDX profiles are inserted in the SEM micrographs [65].

and the predicted value was obtained, indicating the direct oxidation of methane. Park et al. even proved that these Cu/CeO_2–YSZ anodes were active for the direct oxidation of alkanes and alkenes, and when ceria were replaced by SDC catalysts, the anodes were also active for direct oxidation of a wide range of hydrocarbons including aromatics [69].

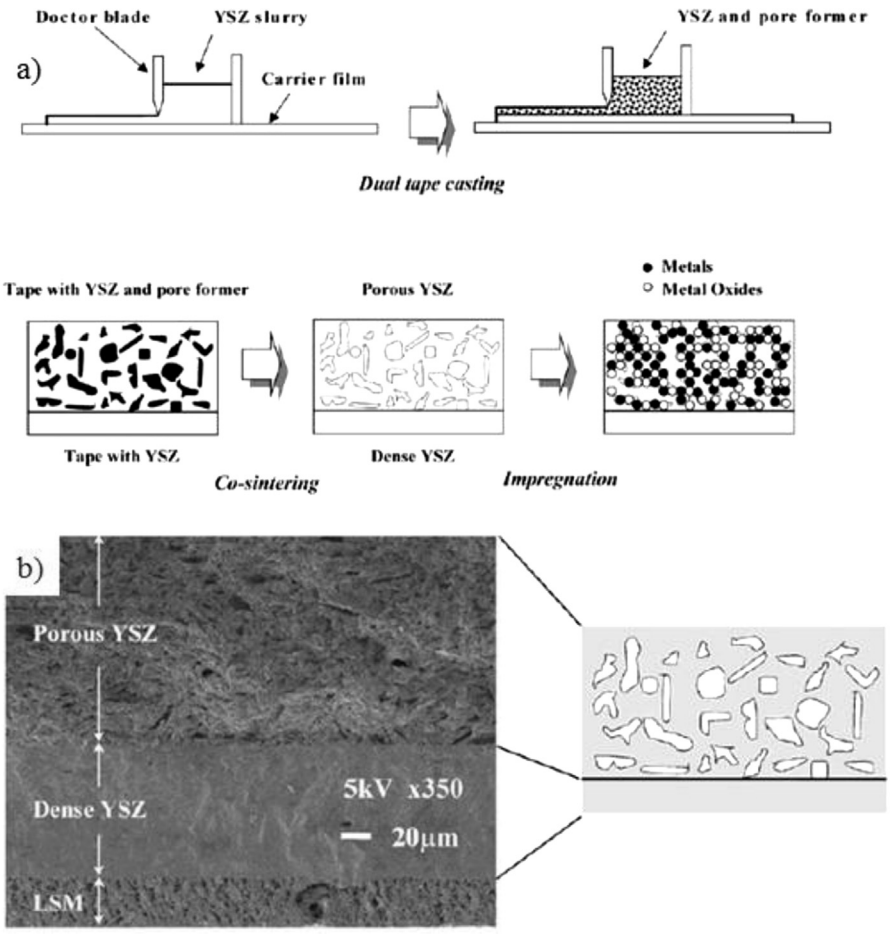

Fig. 10. a) Diagram of the double-layer tape casting procedure used to prepare Cu-impregnated anode-supported SOFC and b) a cross section view of the fabricated cell [70].

The prosperity of Cu-based anodes was greatly accelerated by the development of a double-layer tape casting and subsequent impregnation technique, Fig. 10 [70,71]. This procedure allows the required high temperature sintering for YSZ electrolytes densification, while maintaining sufficient porosity of the anode frameworks for subsequent Cu and catalysts infiltration. The porous YSZ framework can also be prepared by acid leaching the Ni phase out of pre-sintered Ni–YSZ composites [72]. By this method, the porosity of the obtained YSZ structure can be as high as 75% without any collapse. When Cu and catalysts such as ceria were impregnated into porous YSZ backbones, very high performance and stability were obtained, especially with various gaseous (e.g. methane and *n*-butane) and liquid (e.g. toluene, *n*-decane and synthetic diesel) hydrocarbon fuels, Fig. 11 [4,70–75]. Besides YSZ, scandia-stabilized zirconia, DCO and LSGM can also be fabricated as the framework to prepare Cu based anodes with high performance and coking tolerance by infiltration [76–83].

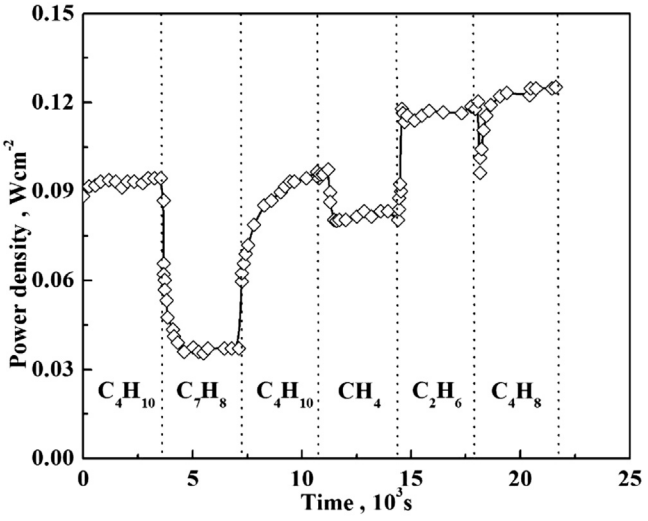

Fig. 11. Effect of switching fuel type (including *n*-butane (C_4H_{10}), toluene (C_7H_8), methane (CH_4), ethane (C_2H_6) and 1-butene (C_4H_8)) on the cell with Cu–SDC impregnated YSZ anode at 700 °C [4].

Besides preparing porous anode framework with dense electrolyte, many efforts were devoted to optimizing the impregnation process of Cu based anodes. It was shown that the cell in which ceria catalyst was added first exhibited better performance than those with Cu first impregnated or Cu/ceria co-impregnated anodes [71]. It was attributed to the fact that in addition to being a good catalyst, ceria was also an oxygen ion conductor, the direct contact between ceria nanoparticles and the YSZ framework increased the effective TPB for electrochemical reaction. He et al. showed that the direct reduction of $Cu(NO_3)_2$ to Cu, resulting in Cu films with better electrical connectivity [84]. Adding urea to aqueous copper nitration solution also exhibited excellent effect of producing a more

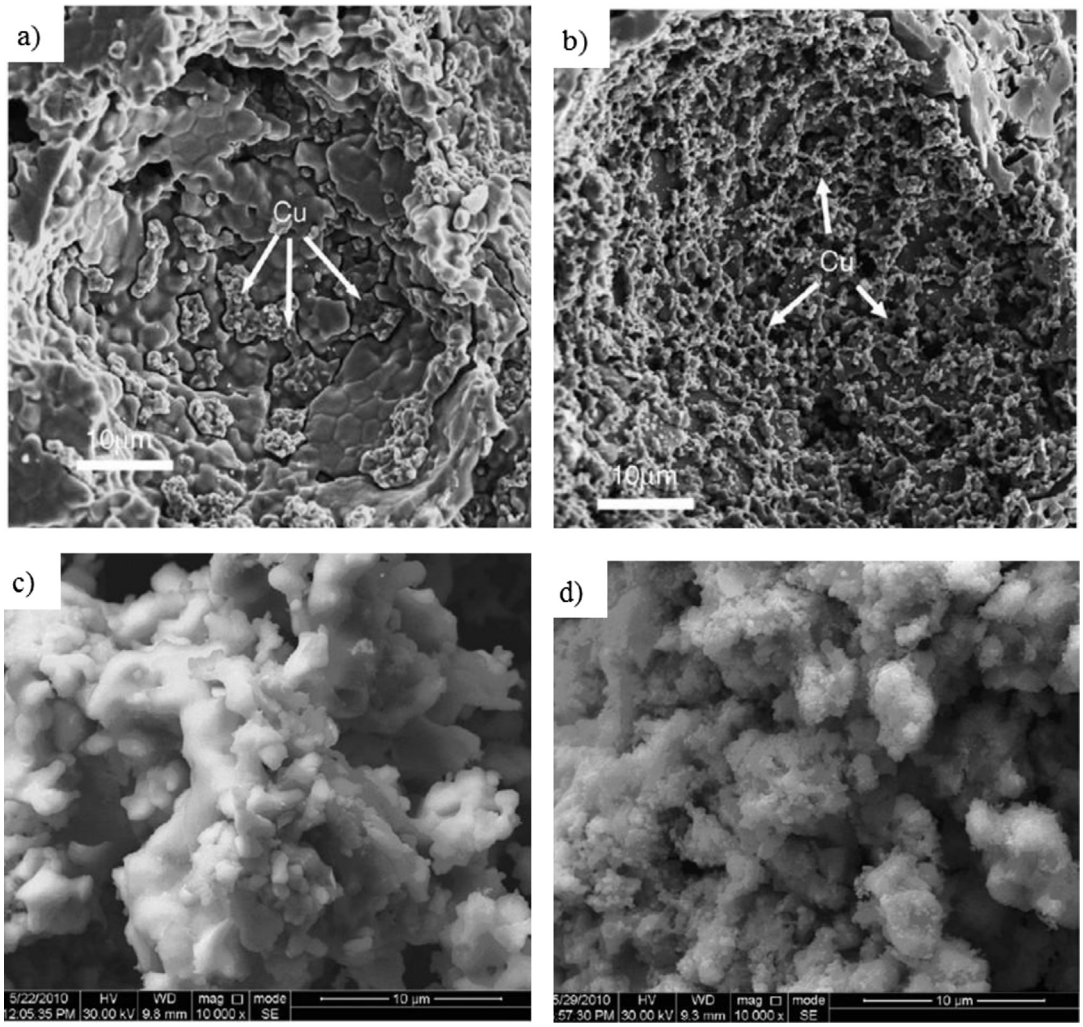

Fig. 12. SEM images of porous YSZ blocks after impregnation of CeO_2 and Cu and subsequent reduction in H_2 at 700 °C for 2 h, a) without and b) with urea added to copper nitrate solution [85]; and SEM images of other Cu–CeO_2/YSZ composite anodes c) without and d) with adding urea after operated in H_2 at 700 °C for more than 10 h [86].

homogenous metal distribution throughout the porous framework, Fig. 12 [85,86].

On the other hand, due to the poor oxidation catalytic activity of Cu itself, additional catalyst such as ceria is essentially required in the anodes, especially for hydrocarbon oxidation. The effect of various lanthanide additives including CeO_2, Eu_2O_3, Tb_4O_7, Pr_6O_{11}, Sm_2O_3, Yb_2O_3, ZrO_2 and La_2O_3 on the performance of Cu–YSZ anodes at 700 °C with H_2 and direct butane was investigated by McIntosh et al. [87]. Among these oxides, ceria was found to be more effective than other lanthanides (Fig. 13), which seemed to be related to the ease with which ceria can be reduced by H_2 and hydrocarbons. Thus, ceria was widely employed as the catalyst for direct utilization of hydrocarbon fuels, even for Cu based anodes or anode functional layers prepared by traditional methods [88–90]. Doping ceria with Yb_2O_3, Y_2O_3, Sm_2O_3, Gd_2O_3, La_2O_3, Nb_2O_5, Ta_2O_5 or Pr_6O_{11}, unfortunately, showed a strong and deleterious effect on the catalytic activity for *n*-butane oxidation [91]. In contrast, replacing CeO_2 with $Zr_{0.4}Ce_{0.6}O_2$ led to improved thermal stability, due to the improved reducibility of the solid solution [92].

Moreover, the addition of Cr or Co by electrodeposition was shown to be beneficial for enhancing the thermal stability of Cu–ceria–YSZ anodes [93,94]. As shown in Fig. 14a, the addition of only 5 vol% Co by electrodeposition exhibited much better thermal stability than those of either Cu–ceria–YSZ, Co–Cu–ceria–YSZ or Co–ceria–YSZ anodes prepared only by impregnation with much higher metal loadings, mainly attributed to the more desirable connectivity of the fabricated metal film. In addition, due to the quick diffusion of Cu through the Co film and the formation of a monolayer Cu on the Co, the Co–Cu–ceria–YSZ anodes by electrodeposition showed excellent tolerance to carbon formation in hydrocarbon fuels, while a Co–ceria–YSZ composite was found to form large amount upon exposure to dry CH_4, Fig. 14b.

An interesting discovery of Cu based anodes was that fuel cells with Cu contents of 20 wt% or lower, large increases were observed in the power densities for operation in H_2 after exposure to any of the hydrocarbons except methane (Fig. 15a) [95]. The enhancement decreased with increasing Cu content, implying that the deposits which did not appear to be graphitic improved the connectivity of the metallic phase in the anode, Fig. 15b. Further investigation proved that the improved conductivity was attributed to the formation of polyaromatic compounds, such as anthracene with rather small amounts [96]. Moreover, these compounds can be

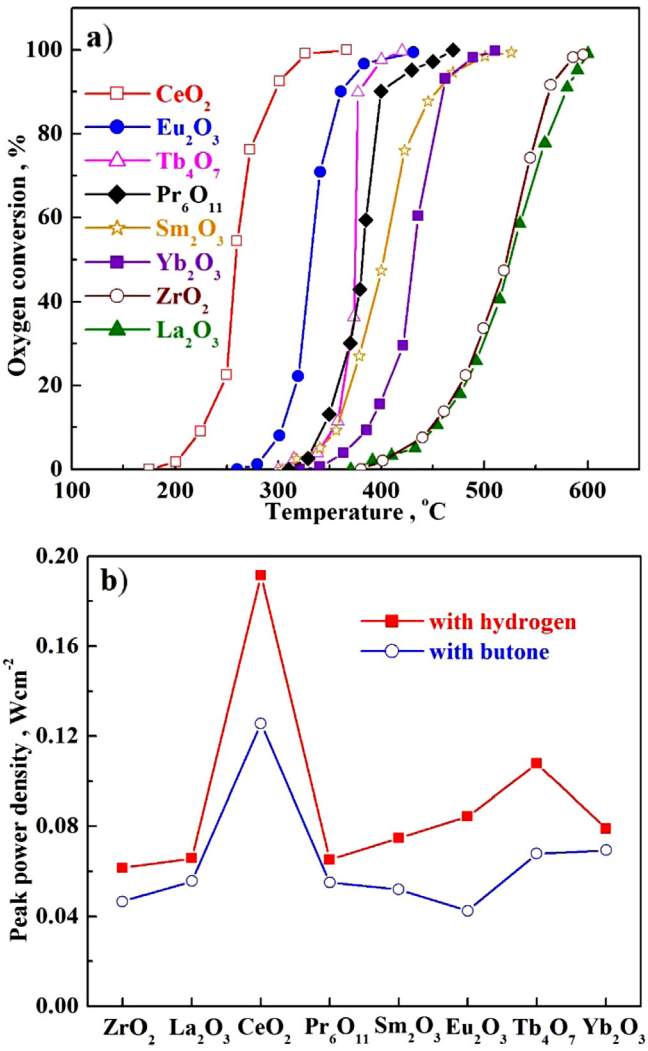

Fig. 13. a) Light-off curves for butane oxidation in 100 Torr of butane and 100 Torr of O_2 with various lanthanide catalysts and b) peak power densities achieved at 700 °C for cells with various lanthanide catalysts added Cu–YSZ anodes [87].

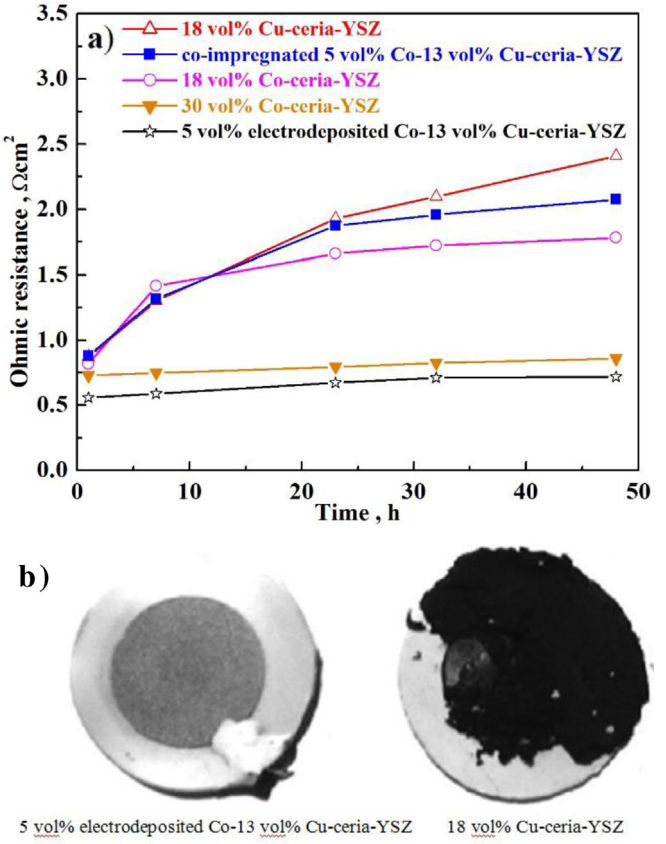

Fig. 14. a) Ohmic resistance measured at 900 °C in humidified H_2 as a function of time for various anodes; b) photos of 5 vol% Co–13 vol% Cu–ceria–YSZ and 18 vol% Co–ceria–YSZ anodes after reduction in dry H_2 and exposure to dry CH_4 for 3 h at 800 °C [94].

easily removed at relatively low temperatures compared with those graphite powders, thus avoiding the adverse effects on the anodes. Accordingly, some carbon–ceria–YSZ anodes without any copper were developed and investigated by exposing only ceria impregnated YSZ matrixes to flowing dry methane at 700 °C for 4 h [96–98].

The sulfur tolerance of Cu-based anodes was also investigated [77,99,100]. As shown in Fig. 16a, H_2 fuel containing H_2S levels up to 450 ppm had no effect on the anode performance, but deactivation was observed at higher H_2S concentrations, which was attributed to the reaction of CeO_2 with H_2S to form Ce_2O_2S [99]. Kim et al. also showed that Cu based anodes could be re-generated by passing steam after being poisoned with higher sulfur levels [100].

3.2. Anodes based on Cu alloys and other metals

While Cu–ceria based anodes exhibited attractive properties, especially their ability for direct utilization of various hydrocarbon fuels, these anodes, however, undergo slow deactivation at temperatures higher than 700 °C due to the low melting point of Cu. As shown above, the addition of Cr or Co by electrodeposition enhanced the thermal stability of Cu–ceria–YSZ anodes [93,94]. Another approach for enhancing the thermal stability as well as the activity of Cu-based anodes involves alloying Cu with a second metal which has much higher melting point and catalytic activity.

Kim et al. examined the use of Cu–Ni alloys as SOFC anodes for the direct oxidation of methane at 800 °C [101]. The performance of a cell with 80% Cu–20% Ni cermet was test in dry methane for 500 h and showed a significant increase in power density with time owing to the enhanced electronic conductivity by small amounts of carbon deposits (Fig. 17a). XRD analysis showed that the Cu–Ni mixtures formed single phase alloys, while Cu–Co bimetallics formed two phase, with Cu covering the surface of most Co [102]. At 700 °C, the addition of both Ni and Co to Cu significantly increased the cell performance with hydrogen fuel, but caused no change in performance for *n*-butane. At 800 °C, improved performance was observed for both H_2 and *n*-butane with Cu–Co bimetallic anode. With humidified (3% H_2O) methane fuel, cells based on Cu–Co mixtures showed improved performance and stability compared to cells prepared with only Cu or Co [103]. In particular, a cell with 50:50 ratio of Cu and Co was shown to be stable for 500 h at 800 °C, Fig. 17b. Costa-Nunes et al. also found that adding Co to Cu–ceria–YSZ anode made the performance on CO even higher than that on H_2 [104]. With Cu–Co(Ru)/ZDC anodes, cells had similar performance and stability in H_2 and methanol, while in ethanol the performance initially increased, and then declined exponentially [105].

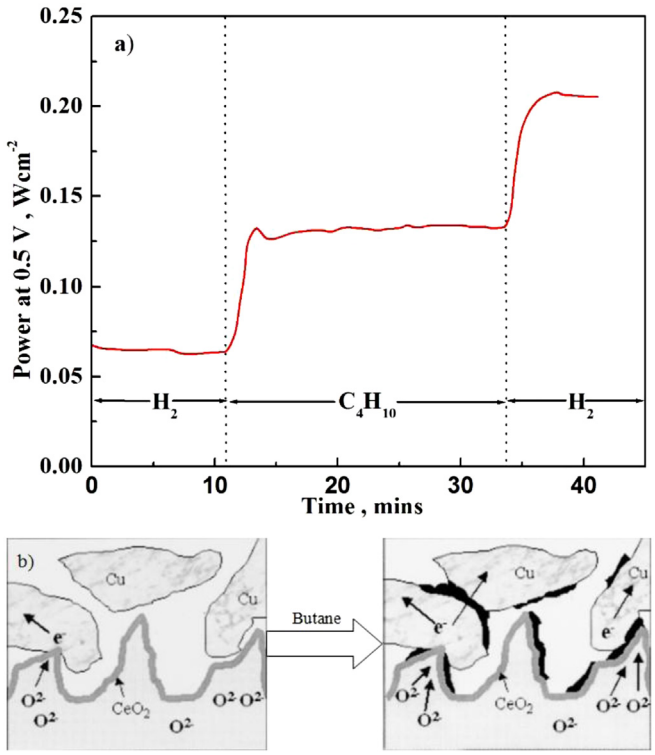

Fig. 15. a) Power density of a cell with 10% CeO_2 and 20% Cu impregnated anode as a function of time at 0.5 V at 700 °C, while the fuel was switched from H_2, to *n*-butane, and back to H_2; b) schematic to describe the changes in the TPB after operation with *n*-butane [95].

This behavior was likely a consequence of carbon deposition that initially improved electronic conductivity of the anode, and subsequently blocked the active sites. Fortunately, the performance could be recovered by re-exposing the anode to humidified hydrogen. Cu–Pd alloys were also impregnated as SOFC anodes, which exhibited equivalent electrochemical performance and even higher carbon tolerance compared to that with pure Pd impregnated ones [106,107].

Besides Cu, Au was also impregnated into SDC frameworks and studied with H_2 and *n*-butane fuels [108]. The similarity of performance curves and impedance spectra for cells with Au and Cu based anodes suggested that both metals were simple electronic conductors in the anodes. Ag impregnated GDC cermets were also shown to be promising anodes for IT-SOFCs using CO as the fuel [109].

4. Novel ceramic anodes fabricated and/or modified by infiltration

Recently, oxide materials which show desirable MIEC have been proposed as novel anodes for SOFCs, such as $La_{1-x}Sr_xCr_{1-y}Mn_yO_{3-\delta}$ (LSCM) [110,111], $La_{1-x}Sr_xCr_{1-y}Fe_yO_{3-\delta}$ (LSCF) [112], $Sr_{1-x}Y_xTiO_{3-\delta}$ [113], and the double perovskite $Sr_2Mg_{1-x}Mn_xMoO_{6-\delta}$ [114]. Ideally, sufficient high MIEC, good redox stability and excellent catalytic activity toward various fuels in particular hydrocarbons oxidation without severe carbon deposition and sulfur poisoning are required for these promising oxides. Actually, however, while each oxides may have some of the desired properties, it is hard to identify a single material which meets all of the requirements mentioned above [115]. Therefore, additional species with specific

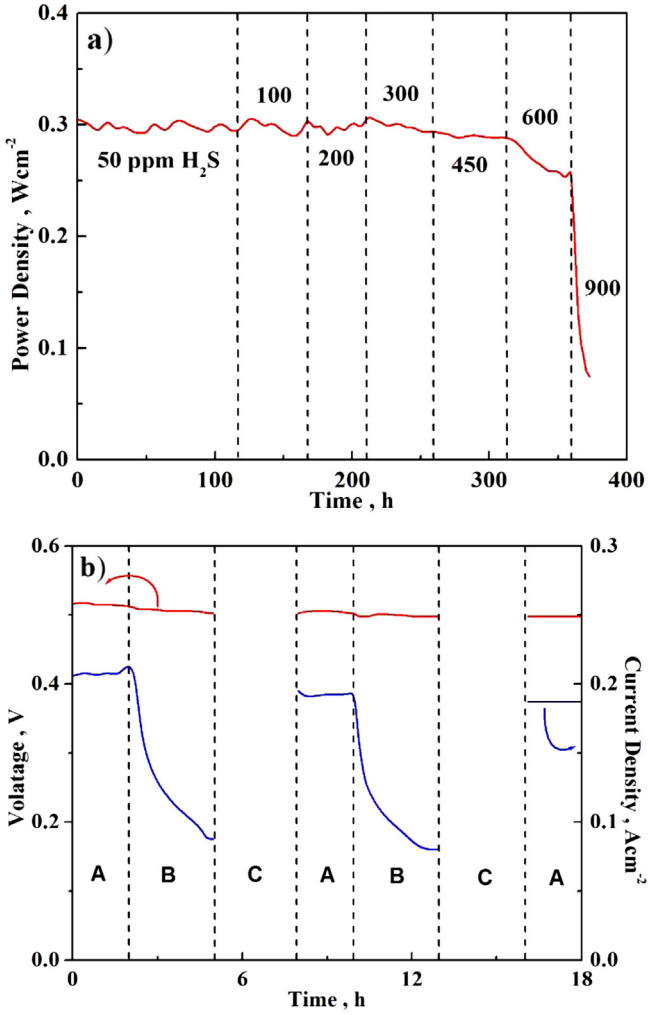

Fig. 16. a) Performance of an SOFC with Cu–ceria–YSZ anode as a function of time at 0.65 V and 800 °C, with H_2S (content as indicated in the figure) + 10 vol% H_2O + H_2 as the fuel [99]; b) performance of a cell with Cu–ceria–YSZ anode as a function of time at 0.5 V and 700 °C, with various fuels: (A) 50 mol% *n*-decane in N_2, (B) 50 mol% *n*-decane + 5000 ppm S and (C) 50 mol% H_2O in N_2 [100].

characteristics are frequently introduced for modification, mainly achieved by means of infiltration.

4.1. $LaCrO_3$ based anodes

$LaCrO_3$ based oxides, which have been investigated as interconnect materials for SOFCs [48], are considered as potential anode materials due to their good stability in both reducing and oxidation conditions at high operation temperatures and very low activity toward carbon deposition [116]. It was shown that Ca and Sr substitution at La site improved the catalytic activity, and for Cr site, Mn, Fe and Ni substitution could improve the activity [117,118].

Among various derivatives, LSCF was shown to be comparable with the Ni–YSZ anodes in wet H_2, thus being considered as a very promising anode for SOFCs [119]. Its catalytic activity for methane steam reforming, however, is very low, even though it does not catalyze the carbon formation, either [120]. Jiang et al. showed that the impregnation of ionic conducting GDC nanoparticles significantly enhanced the catalytic and electrochemical activities for the dry reforming of methane as well as for the electrochemical oxidation reactions of the dry reforming products [121].

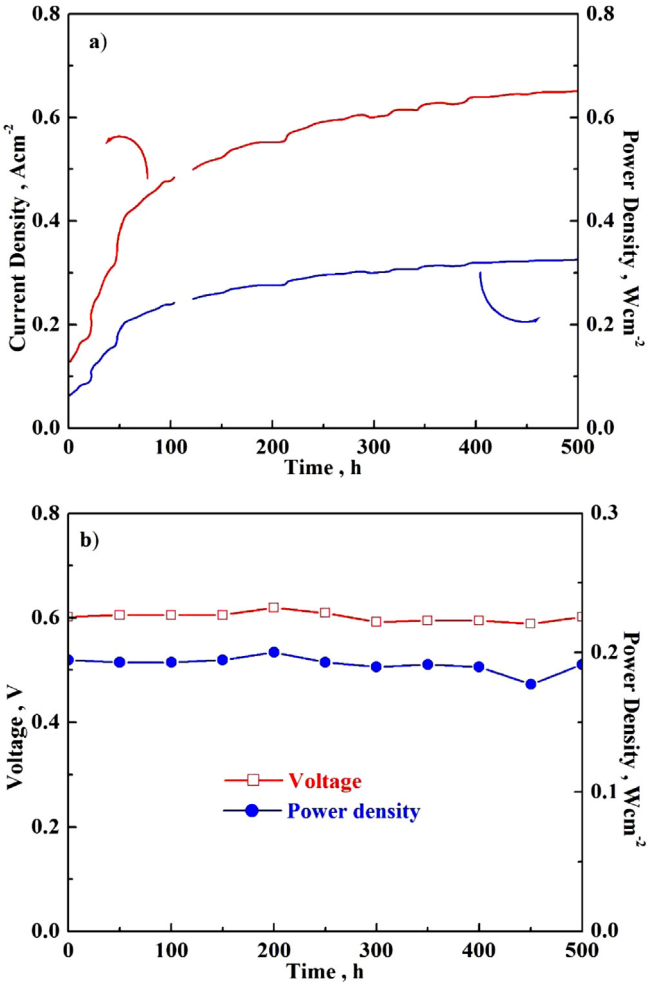

Fig. 17. a) Plots of current density and power density as a function of time at 0.5 V and 800 °C for a cell with 80% Cu–20% Ni anode in 100% methane [101]; b) plots of voltage and power density as a function of time at 800 °C using humidified (3% H_2O) CH_4 for 15 wt% ceria and 30 wt% Cu(50)Co(50) cells [103].

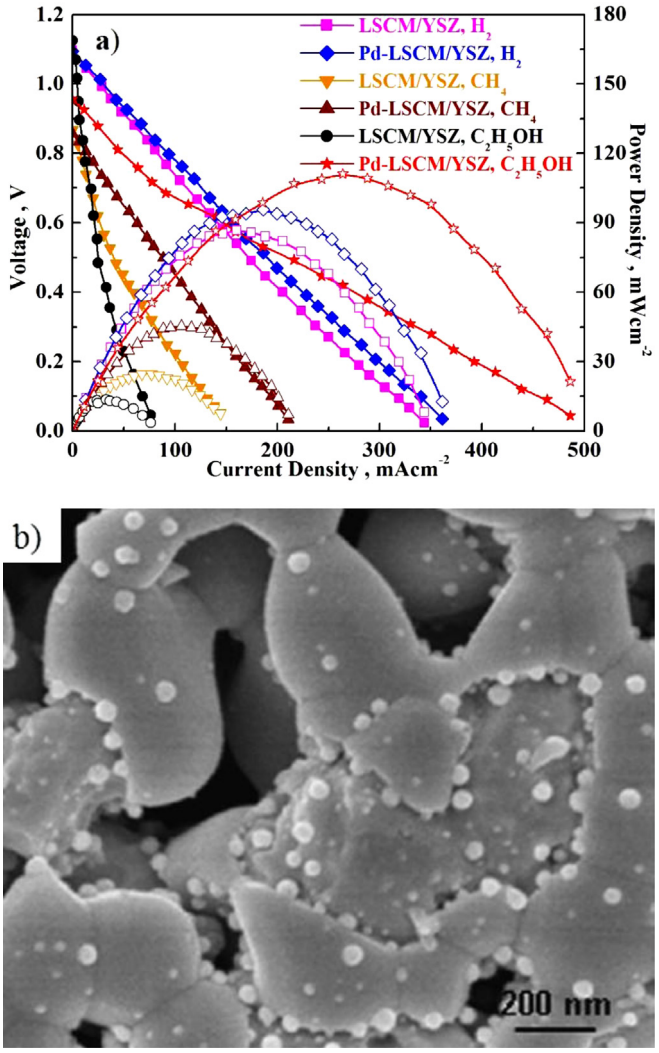

Fig. 18. a) Dependence of cell voltage and power density on current density for cells with LSCM/YSZ and Pd impregnated LSCM/YSZ anodes in H_2, CH_4 and C_2H_5OH at 800 °C; b) scanning electro micrograph of 0.36 mg cm^{-2} Pd impregnated anodes after testing at 800 °C in methane [123].

A similar effect of GDC impregnation on LSCM anodes in humidified methane was proved by Chen et al. with LSM-YSZ cathode supported designs [122].

The impregnation of metallic Pd, Cu and Ni nanoparticles can also enhance the performance of LSCM based anodes. After the impregnation of palladium nanoparticles, the electrocatalytic activity of LSCM/YSZ anodes for the methane and ethanol electro-oxidation reaction was significantly enhanced [123,124]. As shown in Fig. 18a, at 800 °C, the peak power densities were increased by almost two and eight times with methane and ethanol fuels, respectively, after Pd impregnation on LSCM/YSZ anodes. Impedance spectra results indicated that Pd impregnation primarily enhanced the diffusion and dissociation associated with the electrode processes at low frequencies, thereby facilitating the transfer process of reaction species for the electrochemical oxidation reaction of methane and ethanol on LSCM/YSZ anodes. No carbon deposition was observed on the Pd impregnated anodes after testing (Fig. 18b). In contrast, the impregnation of Pd showed little effect on the hydrogen oxidation (Fig. 18a). Since LSCM shows greatly decreased electronic conductivities in reducing atmospheres compared to that in air, the impregnation of Cu significantly enhanced the electronic conductivity of LSCM based anodes [125–127]. Particularly, when 20 wt% Cu and 1.5 wt% Pd were impregnated, the LSCM based anodes exhibited the best performance in both H_2 and CH_4 [125]. Besides, it was shown that the mechanism of methane oxidation on LSCM and Cu impregnated LSCM anodes involved the direct electrochemical oxidation of methane, but when Pd nanoparticles were dispersed on the Cu–LSCM anodes, methane might be firstly catalyzed to form C and H_2, which were subsequently electrochemically oxidized to H_2O and CO_2, respectively. A small amount of Ni or Ni/CeO_2 impregnation also showed positive effect in improving the performance of LSCM based anodes in H_2 and particularly CH_4 fuels without causing carbon deposition [128–130].

Actually, LSCM anode itself can be prepared by impregnating an aqueous nitrate solution containing La^{3+}, Sr^{2+}, Cr^{3+} and Mn^{2+} with the stoichiometric molar ratio into porous YSZ scaffold, as reported in the literature [131–137]. By this method, the formed LSCM–YSZ anodes exhibited a long TPB length due to spreading of the LSCM under oxidizing conditions and then fracturing in reducing atmospheres (Fig. 19) [131,133]. When a small amount of Pd, Pt, Rh, Ni and/or ceria was subsequently added as catalyst, the anodes exhibited much higher performance in H_2 and CH_4

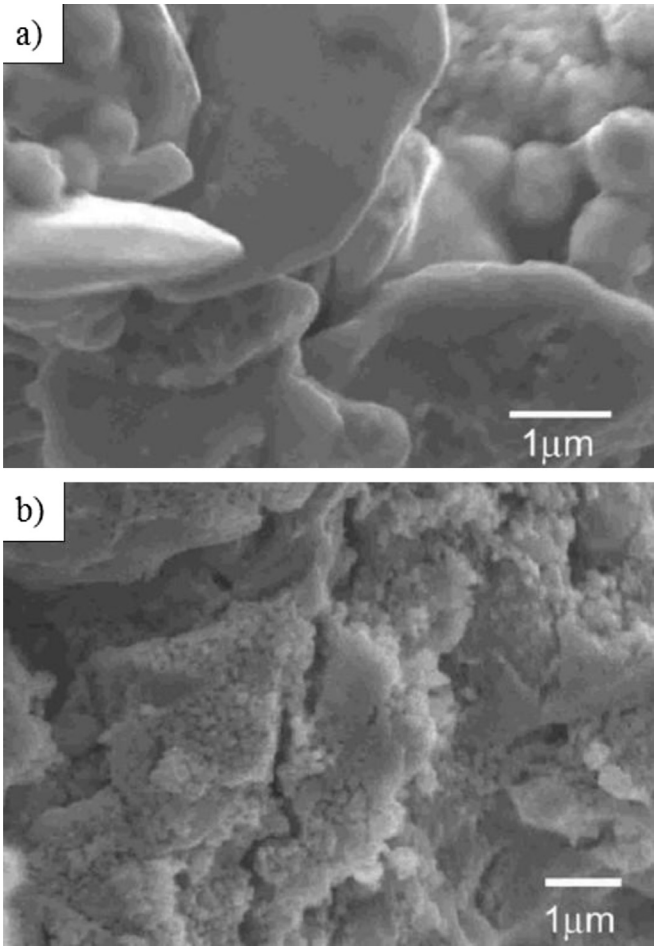

Fig. 19. SEM images of 45 wt% LSCM impregnated YSZ composite a) calcined at 1200 °C in air; b) after reduction in humidified H_2 at 800 °C for 4 h [133].

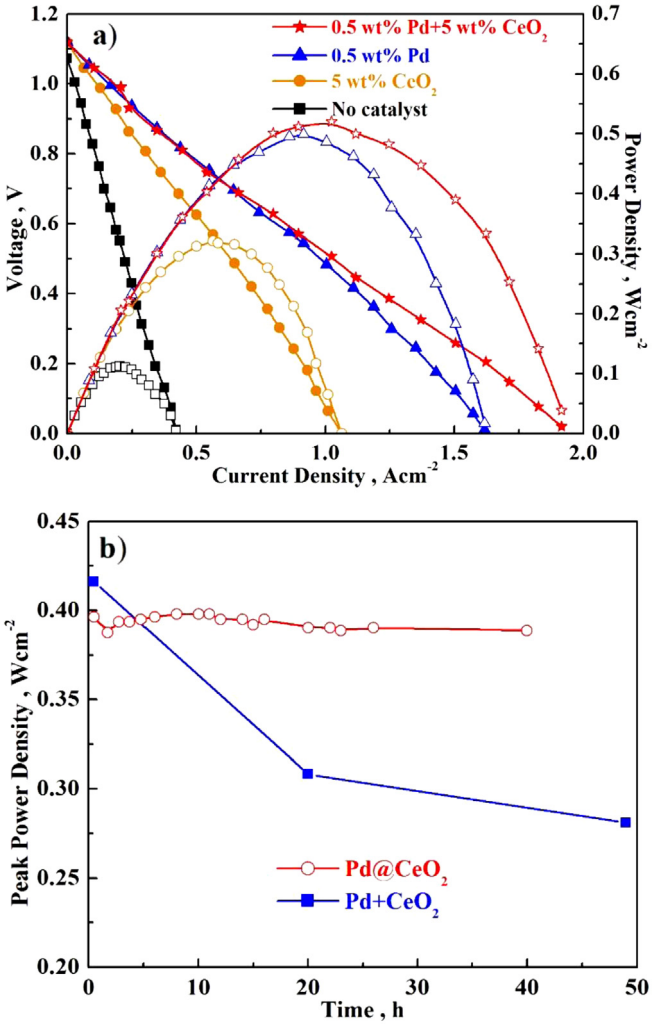

Fig. 20. a) Dependence of cell voltage and power density on current density for cells with 45 wt% LSCM impregnated YSZ anodes using various catalysts in humidified (3% H_2O) H_2 at 700 °C [133]; b) peak power density in humidified (3% H_2O) H_2 at 700 °C as a function of time for cells with LSCM impregnated YSZ anodes using Pd@CeO_2 and Pd + CeO_2 catalyst [135].

fuels [132–137]. As shown in Fig. 20a, the addition of only 0.5 wt % Pd significantly enhanced the performance of LSCM impregnated YSZ anodes in H_2 [133]. On the other hand, although using 5 wt% CeO_2 could also improve the cell performance obviously, the combination of 0.5 wt% Pd and 5 wt% CeO_2 as co-catalyst did not show too much improvement than that using only 0.5 wt% Pd as single catalyst, indicating that 0.5 wt% Pd is sufficient to enhance the catalytic activity of LSCM–YSZ anodes in H_2 fuel. But when CH_4 was used as the fuel, while LSCM–YSZ electrodes containing Pt were very stable, carbon deposits with granular or filamentous morphologies were found on those with either 0.5 wt% Pd or Ni as the catalyst [134]. Fortunately, carbon deposition with both Pd and Ni modified LSCM–YSZ anodes could be greatly suppressed by the addition of 10 wt% ceria as a co-catalyst. It was even found that when Pd@CeO_2 dispersible core-shell structures obtained through self-assembly were infiltrated, the thermal stability of LSCM impregnated YSZ anodes were remarkably improved (Fig. 20b), shown to be the result of greatly suppressed particle-size growth of Pd crystallites [135]. In addition, Zhu and his collaborators proved that the impregnation of a mixture of Ni catalyst and LSCM into porous YSZ backbones was more conducive to fabricate high performance anodes than those impregnating separately [138,139]. A micro-stack consisting of four single cells with LSCM impregnated YSZ anodes was successfully fabricated and operated inside a liquefied petroleum gas flame during coking, showing good properties of carbon-free, redox-stable, quick-start (less than 1 min) and reliable under a wide range of oxygen partial pressure [140].

Sr and Fe doped $LaCrO_3$, LSCF, was also considered as potential SOFC anode materials [112,141,142]. When Ni and SDC nanoparticles were co-impregnated into LSCF anodes, the cell performance in both H_2 and CH_4 was significantly enhanced compared to that with non-modified LSCF anodes [143]. The co-impregnation of LSCF and a small amount of Ni/SDC catalysts into pre-sintered porous YSZ framework was also shown to be an effective approach to fabricate LSCF anodes with outstanding performance and redox stability in H_2, CH_4 and C_2H_5OH fuels (Fig. 21) [144,145]. Other $LaCrO_3$ based oxides such as $La_{0.7}Ca_{0.3}CrO_{3-\delta}$ [146] and $La_{0.7}Ca_{0.3}Cr_{0.5}Mn_{0.5}O_{3-\delta}$ [147] were also investigated as SOFC anodes, whose performance and stability were significantly improved by the impregnation of nano-sized catalyst such as GDC and Pd.

4.2. $SrTiO_3$ based anodes

Among various ceramic materials, doped $SrTiO_3$ was shown to have the highest electrical conductivity in the typical anode

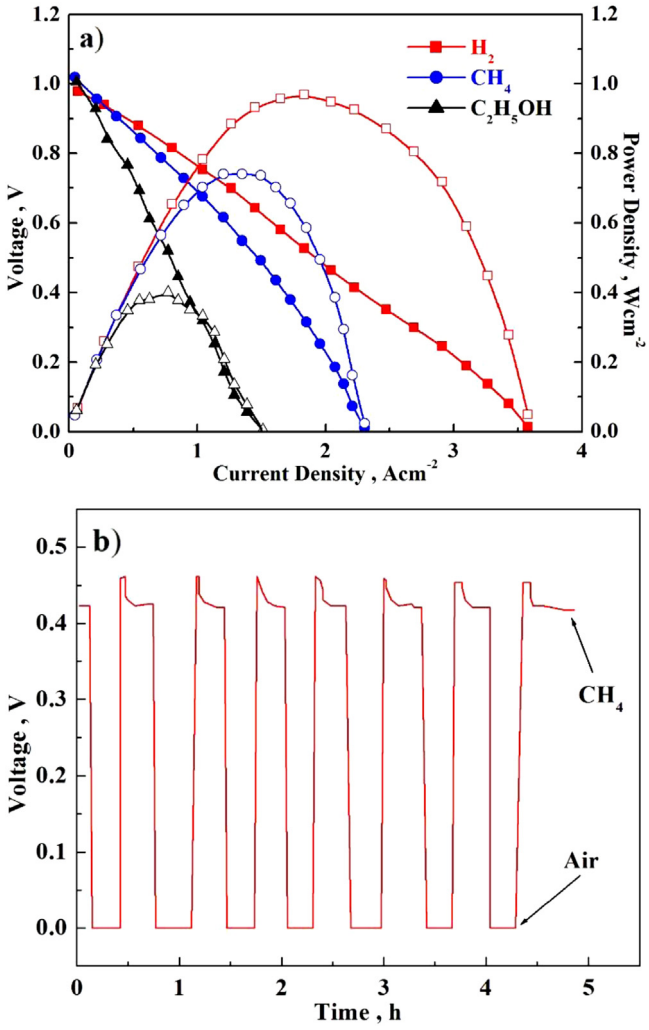

Fig. 21. a) Dependence of cell voltage and power density on current density for cells with LSCrF, Ni/SDC co-impregnated YSZ anodes using H_2, CH_4 and C_2H_5OH as the fuel at 800 °C; b) voltage as a function of time at a constant current density of 1.5 A cm^{-2} for the cell with LSCrF, Ni/SDC co-impregnated YSZ anode over redox cycles between dry CH_4 and air atmosphere at 800 °C [144].

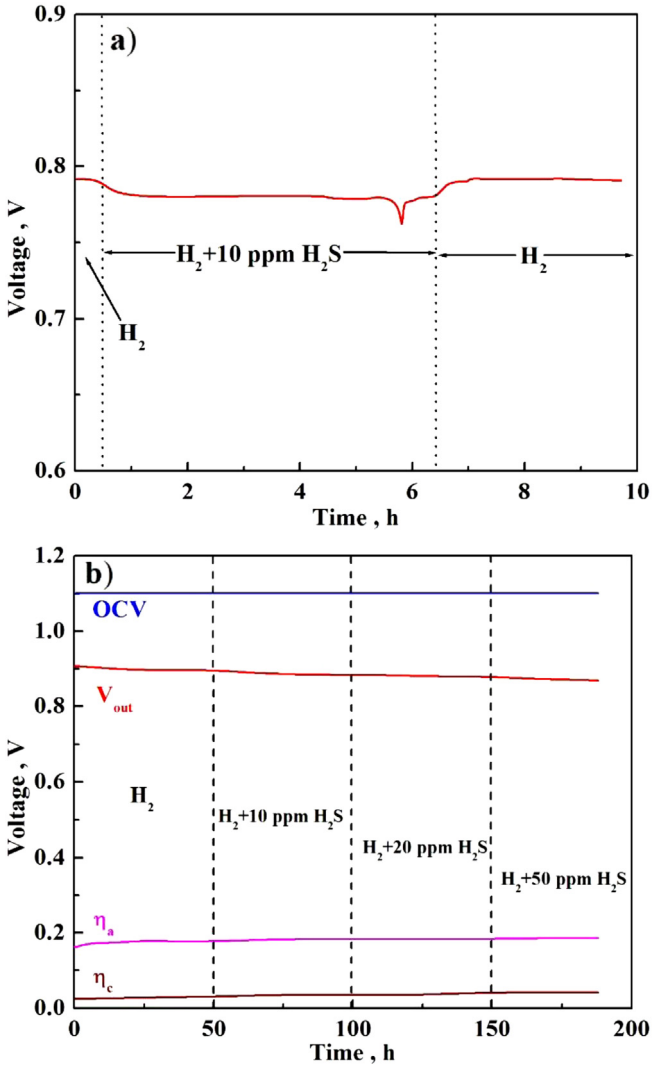

Fig. 22. a) Voltage as a function of time at a constant current density of 0.5 A cm^{-2} for an LSM/YSZ cathode supported cell with Ru/CeO_2 co-impregnated YST/YSZ anode exposed to humidified H_2 containing 10 ppm H_2S at 800 °C [155]; b) the variation of OCV, output voltage, anodic and cathodic overpotential of single cells with Pd impregnated YST/LDC anodes in H_2 and H_2/H_2S fuels under a fixed current density of 417 mA cm^{-2} at 800 °C [156].

environment [148]. Particularly, Hui et al. reported that Y doped $SrTiO_3$ (YST) showed a conductivity as high as 80 S cm^{-1} at 800 °C and oxygen partial pressure of 10^{-14} [149]. When a small amount of Ni catalyst was incorporated into YST/YSZ anodes by infiltration, the electrocatalytic activity was significantly enhanced, without causing detrimental effects on the redox stability of the anodes [150–153]. With 8 wt% Ni impregnated into YST/YSZ and particularly YST/SDC anodes, the cells exhibited remarkably enhanced electrochemical performance under the operation in humidified (3% H_2O) hydrogen and methane fuels, and no performance deterioration was observed over the short-term operation for 20 h in methane [154]. As reported by Kurokawa et al, LSM/YSZ cathode supported cells with Ru and ceria co-impregnated YST/YSZ anodes exhibited good sulfur tolerance when humidified H_2 containing 10–40 ppm H_2S were used as the fuel (Fig. 22a) [155]. Excellent sulfur tolerance was also shown on cells with YST/LDC anodes modified with nano-sized Pd catalysts, Fig. 22b [156]. La doped $SrTiO_3$ and Nb doped $SrTiO_3$ were also considered as promising SOFC anodes, and the incorporation of various additional catalyst was shown to be critical to enhance their performance and stability [157–160], e.g., with the addition of 0.5 wt% Pd and 5 wt% ceria, the peak power density of cells with La doped $SrTiO_3$ impregnated YSZ anodes increased form less than 20 to 780 mW cm^{-2} for operation in humidified (3% H_2O) H_2 at 800 °C [159].

4.3. Other ceramic anodes

Wet impregnation was also widely used to fabricate and/or optimize other alternative ceramic anodes besides doped $LaCrO_3$ and $SrTiO_3$-based oxides. Anodes based on $La_{0.8}Sr_{0.2}Sc_xMn_{1-x}O_{3-\delta}$ infiltrated into YSZ framework were developed and investigated by Sengodan et al., and the additional infiltration of ceria-supported Pd catalyst was shown to be necessary for achieving good performance in humidified methane (Fig. 23) [161,162]. The necessity of impregnating Pd or Pd/CeO_2 nano-sized catalyst to obtain desirable performance and stability was also shown on ceramic anodes based on $La_{0.7}Sr_{0.3}VO_{3.85}$ [163], $Nb_{0.8}WO_3$ [164], $Ce_{0.7}Sr_{0.3}VO_{3.85}$ [165], $SrMoO_3$ [166], etc. Xiao et al. showed that Ni infiltration could promote the oxidation of H_2 on $Sr_2Fe_{1.5}Mo_{0.5}O_6$ based anodes, thus enhancing the cell

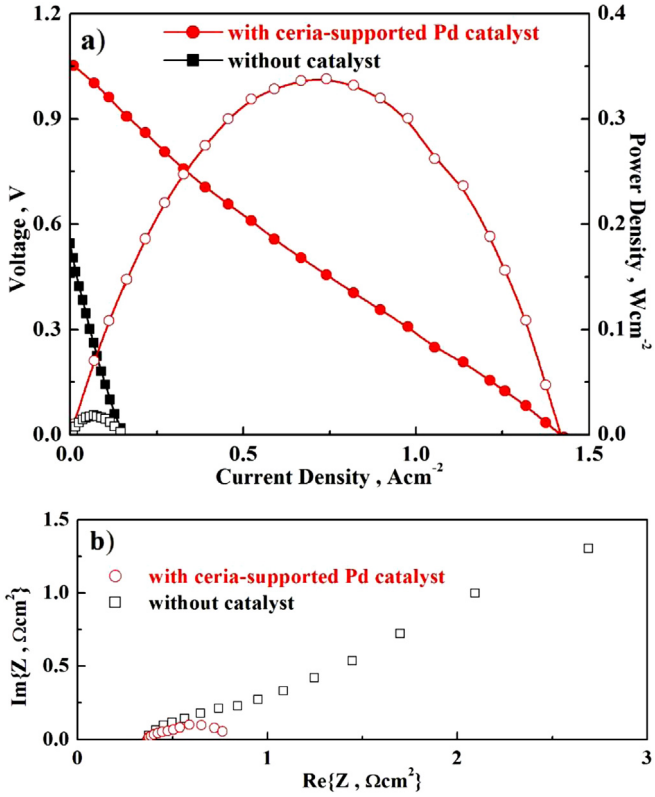

Fig. 23. a) Dependence of cell voltage and power density on current density and b) impedance spectra measured under open circuit conditions, for cells having anodes prepared by infiltration of 40 wt% LSSc0.1 M into YSZ framework with and without ceria-supported Pd catalyst operated in humidified (3% H_2O) fuel at 700 °C [162].

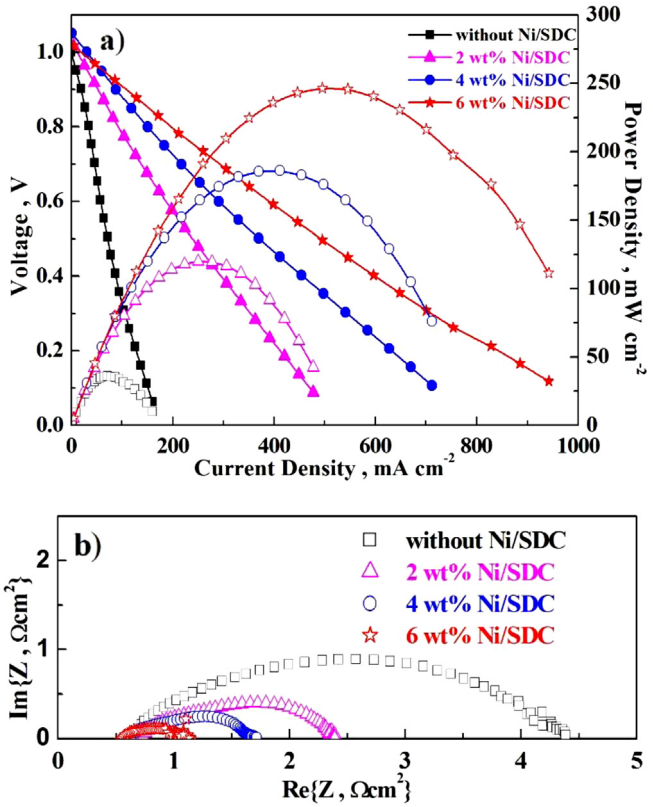

Fig. 24. a) Dependence of cell voltage and power density on current density and b) impedance spectra measured under open circuit conditions, for single cells with Ni–SDC composites impregnated SS430 anodes tested at 700 °C with humidified H_2 (~3% H_2O) as the fuel [173].

performance [129]. The surface exchange coefficient and electrochemical performance of SFM electrodes could also be enhanced by SDC impregnation [167].

5. Metal supported designs

In recent years, there have been lots of interests in developing metal-supported SOFCs, driven by their excellent strength, high tolerance to extremely rapid thermal cycling and redox cycling, as well as low material cost [168]. In such design, the metal support can act as both the support and electronic conducting phase of the anode, and only a small amount of Ni is needed to provide the catalytic activity for fuel oxidation. Five layer structure FeCr metal-supported tubular designs with thin YSZ films and infiltrated Ni and LSM catalysts were developed by Tucker et al. [169]. With these cells, tolerance to five complete redox cycles and five rapid thermal cycles was demonstrated [170]. Planar metal supported cells with Ni/GDC impregnated stainless steel/50 wt% YSZ functional layers were also successfully fabricated, showing fair long-term stability and excellent performance at temperatures around 650 °C [171]. Especially when GDC barrier layers were applied by magnetron sputtering, significantly improved durability with steady degradation rates of 0.9% K h^{-1} in cell voltage for up to 3000 h galvanostatic testing at 650 °C and 0.25 A cm^{-2} was obtained [172]. Liu et al. directly impregnated small amounts of Ni/SDC catalyst into the stainless steel based anode framework of three-layer designs, and the obtained performance increased obviously with the catalyst loading, Fig. 24 [173].

6. Summary and conclusions

Overall, wet impregnation/infiltration is a very effective approach to fabricate and/or optimize SOFC anodes to obtain higher performance and stability, and in principle, any metal oxides which can be synthesized by wet chemical routes can be incorporated into the pre-sintered porous anode scaffold by impregnation to form nanoparticles (for metal species, a subsequent reduction of the oxide is needed). Nano-sized species are impregnated into porous anode framework for two motivations, either to enhance the electronic or ionic conductivity of the electrode or to enhance the catalytic activity, in the case of either or both are not sufficient. When the conductivity, particularly electronic conductivity of the anode scaffold is too low, the impregnated nano-sized species, such as Ni, Cu and LSCM, need to form continuous network or at least be able to connect the originally separated conductive particles. In this case, although some properties especially the redox stability and component compatibility of the anodes are significantly improved, the desired impregnation loading is usually too high. Even with highly porous framework, too much repeated cycles are basically required, thus leading to the complexity and instability for fabrication. For the catalytic activity improvement, Pd and Pd/ceria seem to be the most effective catalyst for both performance and carbon or sulfur tolerance enhancement. However, the cost of Pd or Pd containing compound is too high, making it not the preferred choice for large-scale application. Another concern is the long-term stability of the microstructure and performance of the impregnated anodes. Even though some relatively long time operation with very little degradation is shown in the literature, others also

demonstrated that the particle size of the impregnated species would increase with operation time at high temperatures, subsequently causing the decline in performance.

Fortunately, it is shown that not only the intrinsic properties of the impregnated species, but also the preparation procedures have significant effect on the microstructure and performance of the anodes. Since wet impregnation has proved their feasibility and superiority for preparing high performance nano-structured anodes for small-scale application, as long as more efforts are devoted to the optimization of impregnation procedures as well as the search of novel component materials and catalysts with better characteristics, this technique would be a powerful booster for the large-scale application and commercialization of SOFC technologies.

Acknowledgment

We thank gratefully the financial support of the Ministry of Science and Technology of China (2012CB215403) and the Ministry of Education of China (20113402110014).

References

[1] B.C.H. Steele, A. Heinzel, Nature 414 (6861) (2001) 345–352.
[2] C. Xia, M. Liu, Journal of the American Ceramic Society 84 (8) (2001) 1903–1905.
[3] C. Xia, M. Liu, Solid State Ionics 144 (3–4) (2001) 249–255.
[4] S.D. Park, J.M. Vohs, R.J. Gorte, Nature 404 (6775) (2000) 265–267.
[5] M.L. Toebes, et al., Catalysis Today 76 (1) (2002) 33–42.
[6] S. McIntosh, R.J. Gorte, Chemical Reviews 104 (10) (2004) 4845–4865.
[7] T. Kim, et al., Journal of Power Sources 155 (2) (2006) 231–238.
[8] S. Zha, Z. Cheng, M. Liu, Journal of the Electrochemical Society 154 (2) (2007) B201–B206.
[9] Z. Jiang, C. Xia, F. Chen, Electrochimica Acta. 55 (11) 3595–3605.
[10] S.P. Jiang, et al., Journal of the American Ceramic Society 88 (7) (2005) 1779–1785.
[11] S.P. Jiang, Materials Science and Engineering A 418 (1–2) (2006) 199–210.
[12] S.P. Jiang, International Journal of Hydrogen Energy 37 (1) (2012) 449–470.
[13] R.J. Gorte, J.M. Vohs, Current Opinion in Colloid & Interface Science 14 (4) (2009) 236–244.
[14] M.D. Gross, J.M. Vohs, R.J. Gorte, Journal of Materials Chemistry 17 (30) (2007) 3071–3077.
[15] R.J. Gorte, J.M. Vohs, S. McIntosh, Solid State Ionics 175 (1–4) (2004) 1–6.
[16] W.Z. Zhu, S.C. Deevi, Materials Science and Engineering A – Structural Materials Properties Microstructure and Processing 362 (1–2) (2003) 228–239.
[17] S.P. Jiang, S.H. Chan, Journal of Materials Science 39 (14) (2004) 4405–4439.
[18] S.P. Jiang, Y.Y. Duan and J.G. Love, Journal of the Electrochemical Society 149 (9) 2002, A1175–A1183.
[19] S.P. Jiang, W. Wang, Y.D. Zhen, Journal of Power Sources 147 (1–2) (2005) 1–7.
[20] S.P. Jiang, et al., Electrochemical and Solid State Letters 7 (9) (2004) A282–A285.
[21] B. Timurkutluk, et al., International Journal of Energy Research 35 (12) 1048–1055.
[22] E.V. Tsipis, et al., Journal of Solid State Electrochemistry 8 (9) (2004) 674–680.
[23] S.Z. Wang, et al., Solid State Ionics 174 (1–4) (2004) 49–55.
[24] T.Z. Sholklapper, et al., Nano Letters 7 (7) (2007) 2136–2141.
[25] D. Ding, et al., Journal of Power Sources 179 (1) (2008) 177–185.
[26] W. Zhu, D. Ding, C. Xia, Electrochemical and Solid State Letters 11 (6) (2008) B83–B86.
[27] L. Zhang, et al., Journal of Alloys and Compounds 482 (1–2) (2009) 168–172.
[28] L. Zhang, et al., Journal of the American Ceramic Society 92 (2) (2009) 302–310.
[29] W. Wang, et al., Journal of Power Sources 159 (1) (2006) 68–72.
[30] W. Zhu, et al., Journal of Power Sources 160 (2) (2006) 897–902.
[31] B. Liu, et al., International Journal of Hydrogen Energy 37 (10) 8354–8359.
[32] D. Ding, et al., Electrochemistry Communications 10 (9) (2008) 1295–1298.
[33] Y. Chen, et al., Journal of Power Sources 196 (11) 4987–4991.
[34] H. Kurokawa, et al., Electrochemical and Solid State Letters 10 (9) (2007) B135–B138.
[35] Y. Chen, et al., Journal of Power Sources 204 (15) (2012) 40–45.
[36] Z. Liu, et al., Journal of Power Sources 196 (20) (2011) 8561–8567.
[37] Y. Jin, et al., Electrochemical and Solid State Letters 12 (2) (2009) B8–B10.
[38] Y. Jin, et al., Journal of the Electrochemical Society 157 (1) B130–B134.
[39] H. Yasutake, et al., Journal of the Electrochemical Society 157 (10) B1370–B1375.
[40] L. Liu, et al., Electrochemistry Communications 19 (2012) 63–66.
[41] A. Babaei, S.P. Jiang, Southeast Asian International Advances in Micro/Nanotechnology 7743 (2010) 77430F–1-77430F-10.
[42] A. Babaei, S.P. Jiang, J. Li, Journal of the Electrochemical Society 156 (9) (2009) B1022–B1029.
[43] L.L. Zheng, et al., International Journal of Hydrogen Energy 37 (13) (2012) 10299–10310.
[44] I. Gavrielatos, V. Drakopoulos, S.G. Neophytides, Journal of Catalysis 259 (1) (2008) 75–84.
[45] Z. Wang, et al., Journal of Power Sources 179 (2) (2008) 541–546.
[46] E.N. Armstrong, J.-W. Park, N.Q. Minh, Electrochemical and Solid State Letters 15 (5) (2012) B75–B77.
[47] L. Liu, et al., International Journal of Hydrogen Energy 37 (14) (2012) 10857–10865.
[48] N.Q. Minh, Journal of the American Ceramic Society 76 (3) (1993) 563–588.
[49] S.K. Pratihar, et al., Journal of Power Sources 129 (2) (2004) 138–142.
[50] P. Jasinski, et al., Electrochemical and Solid State Letters 8 (4) (2005) A219–A221.
[51] J. Qiao, et al., Journal of Power Sources 169 (2) (2007) 253–258.
[52] Y. Okawa, Y. Hirata, Journal of the European Ceramic Society 25 (4) (2005) 473–480.
[53] K. Haberko, et al., Journal of Power Sources 195 (17) (2010) 5527–5533.
[54] R.F. Martins, et al., Materials Research Bulletin 44 (2) (2009) 451–456.
[55] V. Petrovsky, et al., Electrochemical and Solid State Letters 8 (7) (2005) A341–A343.
[56] A.N. Busawon, D. Sarantaridis, A. Atkinson, Electrochemical and Solid State Letters 11 (10) (2008) B186–B189.
[57] A. Buyukaksoy, V. Petrovsky, F. Dogan, Journal of the Electrochemical Society 159 (2) (2012) B232–B234.
[58] A. Buyukaksoy, V. Petrovsky, F. Dogan, Journal of the Electrochemical Society 159 (6) (2012) B666–B669.
[59] J.W. Yan, et al., Journal of the Electrochemical Society 149 (9) (2002) A1132–A1135.
[60] J.-E. Hong, et al., International Journal of Hydrogen Energy 36 (22) (2011) 14632–14642.
[61] T. Klemenso, et al., Journal of Power Sources 195 (21) (2010) 7295–7301.
[62] C.H. Law, S.W. Sofie, Journal of the Electrochemical Society 158 (9) (2010) B1137–B1141.
[63] J. Qiao, et al., Fuel Cells 9 (5) (2009) 729–739.
[64] S. Zeng, et al., Journal of Natural Gas Chemistry 19 (5) (2010) 509–514.
[65] M. Cimenti, V. Alzate-Restrepo, J.M. Hill, Journal of Power Sources 195 (13) (2010) 4002–4012.
[66] T.Z. Sholklapper, et al., Fuel Cells 8 (5) (2008) 303–312.
[67] R. Craciun, et al., Journal of the Electrochemical Society 146 (11) (1999) 4019–4022.
[68] S. Park, et al., Journal of the Electrochemical Society 146 (10) (1999) 3603–3605.
[69] S. Park, R.J. Gorte, J.M. Vohs, Applied Catalysis A – General 200 (1–2) (2000) 55–61.
[70] R.J. Gorte, et al., Advanced Materials 12 (19) (2000) 1465–1469.
[71] S. Park, R.J. Gorte, J.M. Vohs, Journal of the Electrochemical Society 148 (5) (2001) A443–A447.
[72] H. Kim, et al., Journal of the American Ceramic Society 85 (6) (2002) 1473–1476.
[73] H. Kim, et al., Journal of the Electrochemical Society 148 (7) (2001) A693–A695.
[74] R.J. Gorte, H. Kim, J.M. Vohs, Journal of Power Sources 106 (1–2) (2002) 10–15.
[75] C. Lu, et al., Solid State Ionics 152 (2002) 393–397.
[76] S. An, et al., Solid State Ionics 175 (1–4) (2004) 135–138.
[77] Z.H. Bi, J.H. Zhu, Electrochemical and Solid State Letters 12 (7) (2009) B107–B111.
[78] C. Lu, et al., Solid State Ionics 175 (1–4) (2004) 47–50.
[79] C. Lu, et al., Journal of the Electrochemical Society 150 (3) (2003) A354–A358.
[80] X.-F. Ye, et al., Journal of Power Sources 164 (1) (2007) 203–209.
[81] X.-F. Ye, et al., Solid State Ionics 180 (2–3) (2009) 276–281.
[82] X.-F. Ye, et al., International Journal of Hydrogen Energy 37 (1) (2012) 505–510.
[83] S.W. Zha, et al., Journal of the Electrochemical Society 151 (8) (2004) A1128–A1133.
[84] H.P. He, J.M. Vohs, R.J. Gorte, Journal of the Electrochemical Society 150 (11) (2003) A1470–A1475.
[85] S.W. Jung, et al., Journal of Power Sources 154 (1) (2006) 42–50.
[86] W. Li, et al., Electrochimica Acta 56 (5) (2011) 2230–2236.
[87] S. McIntosh, J.M. Vohs, R.J. Gorte, Electrochimica Acta 47 (22–23) (2002) 3815–3821.
[88] D.J.L. Brett, et al., Chemical Engineering Science 60 (21) (2005) 5649–5662.
[89] M.D. Gross, J.M. Vohs, R.J. Gorte, Journal of the Electrochemical Society 154 (7) (2007) B694–B699.
[90] Z. Zhan, S.I. Lee, Journal of Power Sources 195 (11) (2010) 3494–3497.
[91] S. Zhao, R.J. Gorte, Applied Catalysis A – General 248 (1–2) (2003) 9–18.
[92] K.Y. Ahn, et al., Electrochemical and Solid State Letters 8 (8) (2005) A414–A417.
[93] M.D. Gross, J.M. Vohs, R.J. Gorte, Journal of the Electrochemical Society 153 (7) (2006) A1386–A1390.
[94] M.D. Gross, J.M. Vohs, R.J. Gorte, Electrochimica Acta 52 (5) (2007) 1951–1957.
[95] S. McIntosh, J.M. Vohs, R.J. Gorte, Journal of the Electrochemical Society 150 (4) (2003) A470–A476.
[96] S. McIntosh, et al., Journal of the Electrochemical Society 151 (4) (2004) A604–A608.

[97] S. McIntosh, J.M. Vohs, R.J. Gorte, Electrochemical and Solid State Letters 6 (11) (2003) A240–A243.
[98] T. Kim, et al., Journal of Power Sources 164 (1) (2007) 42–48.
[99] H.P. He, R.J. Gorte, J.M. Vohs, Electrochemical and Solid State Letters 8 (6) (2005) A279–A280.
[100] H. Kim, J.M. Vohs, R.J. Gorte, Chemical Communications 22 (2001) 2334–2335.
[101] H. Kim, et al., Journal of the Electrochemical Society 149 (3) (2002) A247–A250.
[102] S.I. Lee, J.M. Vohs, R.J. Gorte, Journal of the Electrochemical Society 151 (9) (2004) A1319–A1323.
[103] S.I. Lee, et al., Electrochemical and Solid State Letters 8 (1) (2005) A48–A51.
[104] O. Costa-Nunes, R.J. Gorte, J.M. Vohs, Journal of Power Sources 141 (2) (2005) 241–249.
[105] M. Cimenti, J.M. Hill, Journal of Power Sources 195 (13) (2010) 3996–4001.
[106] Z.H. Bi, J.H. Zhu, Journal of Power Sources 195 (10) (2010) 3097–3104.
[107] J.-T. Zhang, et al., Journal of Power Sources 200 (2012) 29–33.
[108] C. Lu, et al., Journal of the Electrochemical Society 150 (10) (2003) A1357–A1359.
[109] F.-Y. Wang, S. Cheng, B.-Z. Wan, Catalysis Communications 9 (7) (2008) 1595–1599.
[110] S. Tao, J.T.S. Irvine, Journal of the Electrochemical Society 151 (2) (2004) A252–A259.
[111] J. Pena-Martinez, et al., Chemistry of Materials 18 (4) (2006) 1001–1006.
[112] Tao, J.T.S. Irvine, Chemistry of Materials 16 (21) (2004) 4116–4121.
[113] Q.X. Fu, et al., Journal of the European Ceramic Society 28 (4) (2008) 811–820.
[114] Y.-H. Huang, et al., Science 312 (5771) (2006) 254–257.
[115] S. Tao, J.T.S. Irvine, The Chemical Record 4 (2) (2004) 83–95.
[116] H. Yokokawa, et al., Solid State Ionics 52 (1–3) (1992) 43–56.
[117] J. Sfeir, et al., Journal of Catalysis 202 (2) (2001) 229–244.
[118] J. Sfeir, Journal of Power Sources 118 (1–2) (2003) 276–285.
[119] S. Tao, J.T.S. Irvine, Nature Materials 2 (5) (2003) 320–323.
[120] P. Vernoux, et al., Solid State Ionics 135 (1–4) (2000) 425–431.
[121] S.P. Jiang, et al., Journal of the Electrochemical Society 153 (5) 2006, A850–A856.
[122] X.J. Chen, et al., Electrochemistry Communications 9 (4) (2007) 767–772.
[123] S.P. Jiang, et al., Journal of Power Sources 185 (1) (2008) 179–182.
[124] Y. Ye, et al., Journal of the Electrochemical Society 155 (8) (2008) B811–B818.
[125] X.C. Lu, J.H. Zhu, Solid State Ionics 178 (25–26) (2007) 1467–1475.
[126] J. Wan, J.H. Zhu, J.B. Goodenough, Solid State Ionics 177 (13–14) (2006) 1211–1217.
[127] X.-F. Ye, et al., Journal of Power Sources 183 (2) (2008) 512–517.
[128] V.A. Kolotygin, et al., Journal of Solid State Electrochemistry 15 (2) (2011) 313–327.
[129] G.L. Xiao, et al., Journal of Power Sources 201 (1) (2012) 43–48.
[130] X. Zhu, et al., Journal of Power Sources 190 (2) (2009) 326–330.
[131] G. Corre, et al., Chemistry of Materials 21 (6) (2009) 1077–1084.
[132] G. Kim, et al., Electrochemical and Solid State Letters 11 (2) (2008) B16–B19.
[133] G. Kim, et al., Electrochemical and Solid State Letters 12 (3) (2009) B48–B52.
[134] J.-S. Kim, et al., Scripta Materialia 65 (2) (2011) 90–95.
[135] J.-S. Kim, et al., Journal of the Electrochemical Society 158 (6) (2011) B596–B600.
[136] X. Zhu, et al., Journal of Power Sources 196 (2) (2011) 729–733.
[137] X. Zhu, et al., Journal of Power Sources 195 (7) (2010) 1793–1798.
[138] X. Zhu, et al., Electrochimica Acta 55(12) (2010) 3932–3938.
[139] X. Zhu, et al., Journal of the Electrochemical Society 157 (5) (2010) B691–B696.
[140] X. Zhu, et al., International Journal of Hydrogen Energy 37 (10) (2012) 8621–8629.
[141] J. Peña-Martínez, et al., Electrochimica Acta 52 (9) (2007) 2950–2958.
[142] M. Oishi, et al., Journal of Solid State Chemistry 181 (11) (2008) 3177–3184.
[143] X. Zhu, et al., Electrochemical and Solid State Letters 12 (12) (2009) B161–B164.
[144] X. Zhu, et al., Electrochemical and Solid State Letters 13 (8) (2010) B91–B94.
[145] X. Zhu, et al., International Journal of Hydrogen Energy 35 (13) (2010) 6897–6904.
[146] Y. Zhang, et al., International Journal of Hydrogen Energy 36 (5) (2011) 3673–3680.
[147] A. Babaei, et al., Solid State Ionics 181 (25–26) (2010) 1221–1228.
[148] A. Atkinson, et al., Nature Materials 3 (1) (2004) 17–27.
[149] S. Hui, A. Petric, Journal of the Electrochemical Society 149 (1) (2002) J1–J10.
[150] Q. Fu, et al., Journal of Power Sources 171 (2) (2007) 663–669.
[151] Q.X. Fu, F. Tietz, Fuel Cells 8 (5) (2008) 283–293.
[152] T. Ikebe, et al., Journal of the Electrochemical Society 157 (6) (2010) B970–B974.
[153] Q. Ma, et al., Journal of Power Sources 195 (7) (2010) 1920–1925.
[154] P. Puengjinda, et al., Journal of Power Sources 204 (15) (2012) 67–73.
[155] H. Kurokawa, et al., Journal of Power Sources 164 (2) (2007) 510–518.
[156] X.C. Lu, et al., Journal of Power Sources 192 (2) (2009) 381–384.
[157] M.D. Gross, et al., Journal of the Electrochemical Society 156 (4) (2009) B540–B545.
[158] A.M. Hussain, et al., International Journal of Hydrogen Energy 37 (5) (2012) 4309–4318.
[159] S. Lee, et al., Journal of the Electrochemical Society 155 (11) (2008) B1179–B1183.
[160] C.-D. Savaniu, J.T.S. Irvine, Journal of Materials Chemistry 19 (43) (2009) 8119–8128.
[161] S. Sengodan, et al., Journal of the Electrochemical Society 158 (11) (2011) B1373–B1379.
[162] S. Sengodan, et al., Journal of Power Sources 196 (6) (2011) 3083–3088.
[163] J.-S. Park, et al., Journal of Power Sources 196 (18) (2011) 7488–7494.
[164] L. Adijanto, et al., International Journal of Hydrogen Energy 36 (24) (2011) 15722–15730.
[165] L. Adijanto, L., et al., Journal of Solid State Chemistry 190 (2012) 12–17.
[166] B.H. Smith, M.D. Gross, Electrochemical and Solid State Letters 14 (1) (2011) B1–B5.
[167] L. Zhang, et al., Electrochemistry Communications 13 (7) (2011) 711–713.
[168] M.C. Tucker, Journal of Power Sources 195 (15) (2009) 4570–4582.
[169] M.C. Tucker, et al., Journal of Power Sources 171 (2) (2007) 477–482.
[170] M.C. Tucker, et al., Journal of Power Sources 175 (1) (2008) 447–451.
[171] P. Blennow, et al., Fuel Cells 11 (5) (2011) 661–668.
[172] T. Klemenso, et al., Journal of Power Sources 196 (22) (2011) 9459–9466.
[173] Z. Liu, et al., International Journal of Hydrogen Energy 37 (5) (2011) 4401–4405.